Table 3. Protein Expression in HCC and Adjacent Nontumorous Tissue

No	Database Accession No.	Protein Name	Average Mass	Homogeneity Rate (%)	T-test	Score	Coverage (%)	Fold Decrease	References*
N1	gi-24657579	VCL protein (VINCULIN)	116,718	100	0.015	58.3	6.0	1.81	
N2	gi-1709947	Pyruvate carboxylase, mitochondrial precursor	129,533	70	0.007	137.3	10.8	1.70	(14)†
N3	gi-4938304	Lysine-ketoglutarate reductase	102,064	90	<0.001	62.8	6.9	1.55	
N4	gi-19353009	Similar to elongation factor 2b	57,455	100	0.008	30.8	6.2	1.39	
N5	gi-8659555	Aconitase 1	98,318	100	0.008	151.5	18.8	1.39	
N6	gi-31415705	Transferrin	76,981	75	0.006	128.0	17.4	1.60	
N7	gi-40789249	Aspartyl-tRNA synthetase 2 (mitochondrial)	73,498	100	0.011	36.0	9.0	2.13	
N8	gi-12655193	Phosphoenolpyruvate carboxykinase 2 (mitochondrial)	70,635	75	0.025	189.4	20.1	1.86	
N9	gi-11761629	Fibrinogen, alpha chain isoform alpha preproprotein	69,695	80	0.003	86.9	17.9	2.07	
N10	gi-284351	Phosphoglucomutase	61,352	89	0.004	38.8	6.0	1.48	
N11	gi-4758312	Electron-transferring-flavoprotein dehydrogenase	68,489	89	0.004	82.6	12.3	1.48	
N12	gi-4557645	Heterogeneous nuclear ribonucleoprotein L isoform a	60,169	100	0.007	41.7	10.4	1.74	
N13	gi-20149621	Hypothetical protein LOC26007	58,892	100	0.001	168.6	35.1	2.29	
N14	gi-4557014	Catalase	59,700	89	0.010	161.6	15.4	1.62	(15)†
N15	gi-11140815	Formiminotransferase cyclodeaminase	58,871	100	0.004	158.6	20.3	2.26	
N16	gi-7431380	Uridine diphosphoglucose dehydrogenase	55,040	100	0.032	31.0	7.7	1.31	
N17	gi-4507813	UDP-glucose dehydrogenase	54,971	100	0.032	50.0	12.4	1.31	
N18	gi-4503375	Dihydropyrimidinase	56,575	100	0.032	60.7	8.7	1.31	
N19	gi-25108887	Aldehyde dehydrogenase family 7 member A1	55,348	78	0.003	25.2	6.0	1.71	
N20	gi-4885281	Glutamate dehydrogenase 1	61,379	100	<0.001	181.0	26.8	1.42	
N21	gi-13027638	UDP-glucose pyrophosphorylase 2 isoform a	56,947	100	<0.001	119.6	23.4	2.37	
N22	gi-7705688	Leucine aminopeptidase	56,031	100	<0.001	94.0	17.4	2.44	
N23	gi-28949044	Human mitochondrial aldehyde dehydrogenase	54,426	100	0.023	101.3	15.2	1.49	(16)
N24	gi-20151189	Human glutamate dehydrogenase-apo form	55,990	100	<0.001	181.0	26.8	1.74	
N25	gi-16306550	Selenium binding protein 1	52,339	100	0.010	90.0	18.8	1.42	
N26	gi-22547189	Serine hydroxymethyl transferase 1 (soluble) isoform 2	48,978	89	0.010	89.7	22.1	2.30	
N27	gi-4503481	Eukaryotic translation elongation factor 1 gamma	50,100	100	0.001	30.9	5.8	2.23	
N28	gi-6730018	Human L-arginine:glycine amidinotransferase	44,625	100	0.001	163.7	26.5	2.23	
N29	gi-5031751	3-Hydroxy-3-methylglutaryl-coenzyme A synthase 2	56,581	80	0.007	170.1	22.1	1.66	
N30	gi-19743875	Fumarate hydratase precursor	54,619	89	<0.001	121.0	27.2	2.31	
N31	gi-16878083	Enolase 3	46,884	89	<0.001	49.3	12.4	2.31	
N32	gi-4557888	Keratin 18	48,010	86	0.037	134.9	18.2	1.41	(17)
N33	gi-16950633	Argininosuccinate synthetase	46,482	100	<0.001	84.4	16.9	3.58	(18)†
N34	gi-4530461	Betaine-homocysteine methyltransferase	44,980	100	<0.001	139.0	33.4	5.19	
N35	gi-28178832	Isocitrate dehydrogenase 2 (NADP+), mitochondrial	50,891	90	0.001	110.0	27.0	2.09	
N36	gi-4557587	Fumaryl acetoacetate hydrolase (fumary lacetoacetase)	46,326	100	0.001	106.5	24.1	2.17	(19)
N37	gi-7110715	SEC14-like 2	46,127	89	0.038	83.3	17.6	1.69	
N38	gi-12804931	Acetyl-coenzyme A acyltransferase 2	41,906	100	0.001	119.4	29.4	2.27	
N39	gi-7542837	Medium-chain acyl-CoA dehydrogenase	46,570	88	<0.001	88.6	18.4	1.71	
N40	gi-4557237	Acetyl-coenzyme A acetyltransferase 1 precursor	45,181	78	<0.001	138.4	35.3	1.90	
N41	gi-4501853	Acetyl-coenzyme A acyltransferase 1	44,273	71	0.046	56.7	9.3	1.68	
N42	gi-4504067	Aspartate aminotransferase 1	46,229	100	0.018	95.7	21.7	2.00	
N43	gi-3337390	Haptoglobin	38,215	100	0.001	34.5	8.0	1.74	(20)
N44	gi-4501929	Class I alcohol dehydrogenase, alpha subunit	39,840	88	<0.001	121.2	23.0	4.12	
N45	gi-494091	Chain A, alcohol dehydrogenase (beta-1 isoenzyme)	39,606	100	0.019	84.8	20.4	3.67	
N46	gi-20530221	BLOCK 25	37,747	80	0.029	30.0	18.8	2.34	
N47	gi-13096743	Chain A, human gamma-2 alcohol dehydrogenase	39,676	100	<0.001	106.6	20.9	4.21	
N48	gi-25777615	Proteasome 26S non-ATPase subunit 7	37,007	80	0.006	21.4	7.3	1.86	(21)
N49	gi-1352403	Fructose-1,6-bisphosphatase 1	36,810	100	<0.001	150.4	43.9	2.28	
N50	gi-4507155	Sorbitol dehydrogenase	38,293	90	0.005	69.2	21.9	2.06	
N51	gi-113611	Fructose-bisphosphate aldolase B (liver-type aldolase)	39,455	100	0.003	137.9	28.2	2.59	
N52	gi-1705823	Aldo-ketoreductase family 1 member C4	37,097	100	0.045	110.0	26.6	1.38	(21)
N53	gi-688031	Aryl sulfotransferase ST1A3	34,191	89	0.003	30.4	11.8	2.63	
N54	gi-8815565	Alcohol/hydroxysteroid sulfotransferase	33,747	89	0.003	29.3	8.6	2.63	
N55	gi-9506741	Glycine N-methyltransferase	32,724	75	0.004	42.4	13.6	2.28	
N56	gi-12654663	Esterase D/formylglutathione hydrolase	31,502	75	0.004	56.5	22.1	2.28	
N57	gi-9087220	Sulfotransferase 1A1 (arylsulfotransferase 1)	34,179	100	0.009	84.0	28.6	2.01	
N58	gi-17402865	Thiosulfate sulfurtransferase (rhodanese)	33,410	100	<0.001	99.5	28.2	1.58	
N59	gi-4503607	Electron transfer flavoprotein, alpha polypeptide	35,061	90	<0.001	120.8	43.9	1.72	
N60	gi-4503301	2,4-Dienoyl CoA reductase 1 precursor	36,049	89	0.004	91.5	24.2	1.76	

*The references can be found in Supplementary Information 2.

†Previously reported to be down-regulated in HCC.

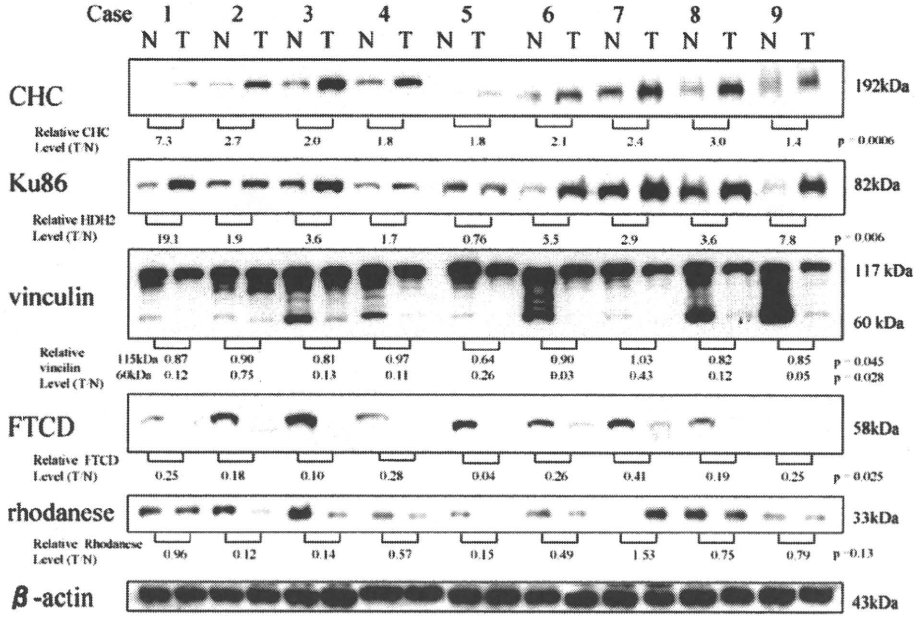

Fig. 2. Immunoblot analysis of differential protein expression in tumor tissues. Total protein lysates prepared from nine matched samples of tumor (T) and adjacent nontumor tissue (N) were separated by electrophoresis on 10% to 20% polyacrylamide gradient gel, and immunoblotted with anti-clathrin heavy chain (CHC) antibody, anti-82 kDa adenosine triphosphate-dependent DNA helicase II (Ku86) antibody, anti-vinculin antibody, anti-formiminotransferase cyclodeaminase (FTCD) antibody, anti-rhodanese antibody, and anti-β-actin antibody (loading control). The intensity of each band was measured with NIH Image, and these proteins levels between tumor and nontumor tissue, normalized with β-actin, were calculated. The expressions of CHC and Ku86 were increased in tumor tissues, whereas vinculin, FTCD, and rhodanese were decreased in tumor tissues.

86.7% and 95.6% when glypican-3 was used with FTCD. These results indicate that combination of the three markers greatly improves the diagnostic accuracy of HCC.

It has recently been recommended to perform a biopsy to identify the features of malignancy when small hepatic masses are detected. As a result, a distinction among regenerative, dysplastic, and malignant hepatocellular nodules is needed on liver biopsy specimens. Therefore, we tested whether we can distinguish eHCC from benign tumors such as dysplastic and regenerative nodules. A total of 18 eHCC tissues and 10 benign tumor tissues (five FNH, three LRN, and two adenomas) were immunostained with CHC, FTCD, and glypican-3 antibodies (Table 6). Note that high-grade dysplastic nodules were included in eHCC because they have been considered as premalignant or malignant lesions by abnormally increased arteriolar and capillary supply.[18] In contrast, low-grade dysplastic nodules were included in benign tumor. Seven eHCCs were distinguished from adjacent nontumor tissues by stronger staining of CHC, whereas one of FNH and LRN was weakly stained with CHC antibody (Fig. 5A, Table 6). Eight eHCCs showed weaker staining of FTCD than adjacent nontumor tissues (Fig. 5B, Table 6). In contrast, all of the FNH and LRN tissues were moderately stained, which is indistinguishable from their adjacent nontumor tissues. Two adenoma tissues showed weaker staining of FTCD than nontumor tissues. Six eHCCs and none of the benign tumors showed stron-

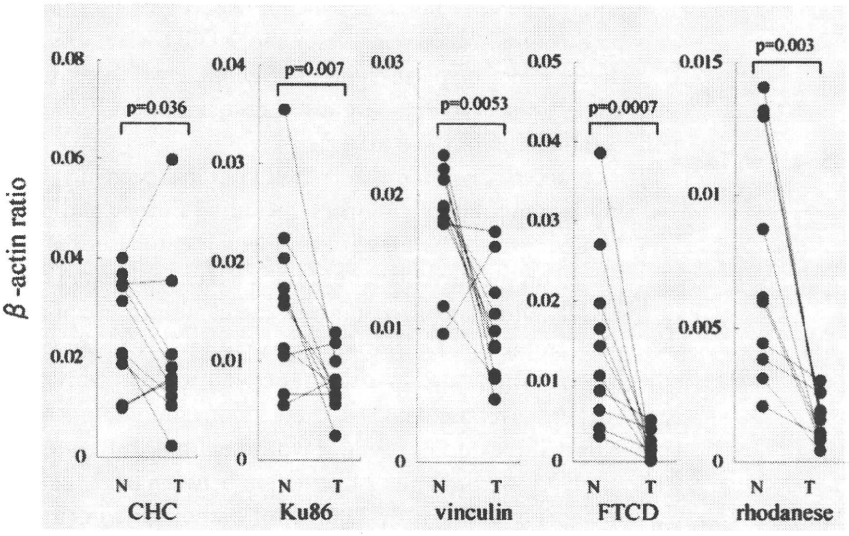

Fig. 3. Quantification of mRNA levels in tumor tissues. Total RNAs were prepared from nine matched samples of tumor (T) and adjacent nontumor tissue (N), and real-time quantitative reverse transcription polymerase chain reaction of CHC (clathrin heavy chain), Ku86 (anti-82-kDa ATP-dependent DNA helicase II), vinculin, FTCD (formiminotransferase cyclodeaminase), and rhodanese mRNA was performed using a LightCycler. These mRNA levels were normalized by β-actin level.

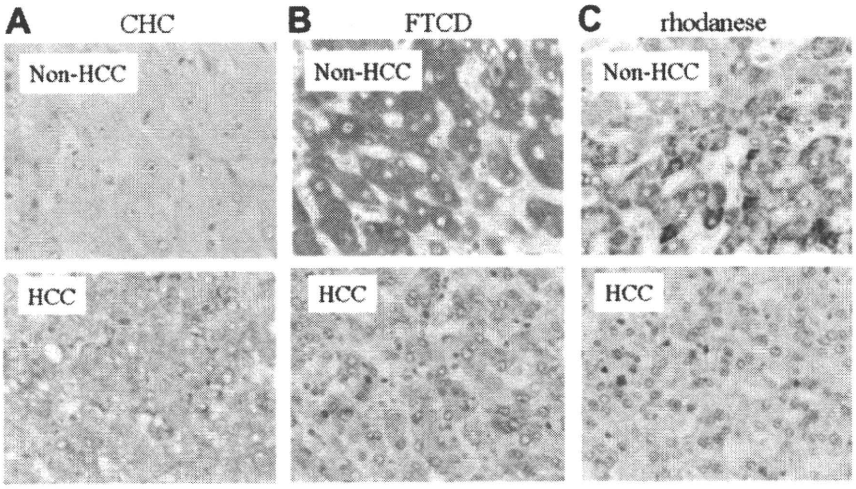

Fig. 4. Immunohistochemical analyses of differential protein expression in tumor tissues. From HCC specimens, paraffin-embedded blocks of tumor and adjacent nontumor tissue were collected. Four-micron sections from paraffin tissue were fixed on slide glasses. The primary antibody is equal to immunoblot analysis. EnVision + system was used to visualize tissue antigens, and tissue sections were counterstained with hematoxylin. (A) Although no staining of CHC (clathrin heavy chain) was observed in nontumor tissues, tumor cells showed scattered staining in the cytoplasm and plasma membrane. (B) FTCD (formiminotransferase cyclodeaminase) showed strong and uniform staining in the cytoplasm of nontumor tissue compared with faint staining in the cytoplasm of tumor cells. (C) Rhodanese showed a mixture of scattered and strong staining in the cytoplasm of nontumor tissue, whereas tumor tissue was scarcely stained.

ger staining of glypican-3 than adjacent nontumor tissues. The sensitivity and specificity of CHC, FTCD, and glypican-3 individually for detection of early HCC was 41.2% and 77.8% for CHC, 44.4% and 80.0% for FTCD, and 33.3% and 100% for glypican-3 (Table 6). The sensitivity of CHC or FTCD was better than that of glypican-3. Moreover, the sensitivity significantly increased by combination of these markers, 72.2% for CHC + FTCD, 61.1% for CHC + glypican-3 and FTCD + glypican-3. This is because 44% of glypican-3–negative eHCCs were able to be detected by either CHC or FTCD staining. These results support that CHC and FTCD are potential biomarkers for early detection of HCC.

Table 4. Histology of HCC and Non-HCC Tissues on Tissue Array

	Histology	Case
HCC tissue	Well-differentiated HCC	14
	Moderately differentiated HCC	40
	Poorly differentiated HCC	11
	Unclassified	18
Non-HCC tissue	Chronic hepatitis	8
	Cirrhosis	19
	Dysplastic nodule	1
	Nonspecific reactive change	11
	Reactive hepatitis	20
	Unknown	9

Discussion

In this study, we compared protein expressions between HCC and adjacent nontumor tissues using a proteome method. A total of 83 proteins with altered expression were identified. Validation of the differentially expressed protein by immunoblot or immunostaining demonstrates that CHC, Ku86, FTCD, rhodanese, and vinculin showed striking differences between tumor and nontumor tissues. Evaluation of the staining intensity of CHC and FTCD enabled us not only to distinguish nontumor and tumor tissues with high accuracy but to discriminate eHCC and benign tumors such as dysplastic and regenerative nodules, which is challenging for expert pathologists. Moreover, CHC and FTCD were able to detect several glypican-3–negative eHCCs, which considerably improved the diagnostic accuracy of eHCC by combination of these markers.

In recent years, the incidence of HCC has been increasing in a number of countries, including Europe and the United States.[19] As a result, considerable emphasis is now placed on the surveillance of HCC. Recent guidelines for HCC management recommend the combined use of alpha-fetoprotein and ultrasonography for HCC surveillance.[7] When small hepatic masses of 1 to 2 cm within a cirrhotic liver are detected, these lesions should undergo biopsy if they do not exhibit typical radiological features of HCC. Accordingly, a distinction between benign and malignant tumor is demanded for pathologists in small

Table 5. Immunohistochemical Analysis From Tissue Array of HCC

A

	CHC		FTCD		Glypican-3	
Expression	Non-HCC	HCC	Non-HCC	HCC	Non-HCC	HCC
3	3	43	45	12	0	38
2	27	33	22	20	2	14
1	31	6	1	32	49	13
0	7	1	0	19	17	18

B

	HCC (n = 83)		Non-HCC (n = 68)		Sensitivity (%)	Specificity (%)
	+	−	+	−		
CHC = 3	43	40	3	65	51.8	95.6
FTCD ≤ 1	51	32	1	67	61.4	98.5
Glypican-3 ≥ 2	52	31	2	66	62.7	97.1
CHC = 3 or FTCD ≤ 1	67	16	4	64	80.7	94.1
CHC = 3 or Glypican-3 ≥ 2	59	24	6	62	71.1	91.2
FTCD ≤ 1 or Glypican-3 ≥ 2	72	11	3	65	86.7	95.6

C

	CHC				FTCD			
Expression	Non-HCC	Well	Moderate	Poor	Non-HCC	Well	Moderate	Poor
3	3 (4.4%)	3 (21.4%)	21 (52.5%)	8 (72.7%)	45 (66.2%)	4 (28.6%)	6 (15.0%)	1 (9.1%)
2	27 (39.7%)	6 (42.9%)	18 (45.0%)	3 (27.3%)	22 (32.4%)	4 (28.6%)	9 (22.5%)	4 (36.4%)
1	31 (45.6%)	4 (28.6%)	1 (2.5%)	0 (0%)	1 (1.5%)	4 (28.6%)	16 (40.0%)	4 (36.4%)
0	7 (10.3%)	1 (7.1%)	0 (0%)	0 (0%)	0 (0%)	2 (14.3%)	9 (22.5%)	2 (18.2%)

biopsies, and further immunohistochemical markers with sufficient sensitivity and specificity are desired. Some markers that can distinguish HCC from dysplastic nodules in cirrhosis have recently been reported.[17] The diagnostic yield of three putative HCC markers, HSP70, glypican 3, glutamine synthetase, was investigated; these were previously proposed by other researchers as promising markers for HCC. However, we identified two novel proteins, CHC and FTCD, by comprehensive proteome analysis, and they were found to be useful for the pathological diagnosis of HCC. Diagnostic values, such as the sensitivity and specificity of proteins for HCC, are comparable to glypican-3 in our analyses. More importantly, the sensitivity and specificity significantly increased when immunostaining of glypican-3 was used with that of CHC and FTCD. Thus, a combination of these markers is useful for screening of HCC.

Table 6. Immunohistochemical Analysis of CHC, FTCD, and Glypican 3 in Early HCC Tissues

	Early HCC		Benign Tumor			
	T > N or T < N	T = N	T > N or T < N	T = N	Sensitivity (%)	Specificity (%)
CHC	7	10	2	7	41.2	77.8
FTCD	8	10	2	8	44.4	80.0
Glypican-3	6	12	0	10	33.3	100

T, tumor tissues; N, nontumor tissues.

Overexpression of CHC in HCC was confirmed by immunoblotting, and most HCC showed strong and scattered staining in the cytoplasm and plasma membranes. Although CHC overexpression has not been reported in any other primary human cancers, fusion of the CHC gene to other genes, such as ALK and TFE3, has been documented in large B-cell lymphoma, pediatric renal adenocarcinoma, and inflammatory myofibroblastic tumor.[20-24] These results indicate that deregulated expression of CHC might play important roles for tumorigenesis. CHC is known to be localized in the plasma membrane and the cytoplasmic face of intracellular organelles in the plasma membrane, called coated vesicles and coated pits. These specialized organelles are involved in the intracellular trafficking of receptors and endocytosis of a variety of macromolecules.[25] Recently, Royle et al.[26] showed that clathrin stabilizes fibers of the mitotic spindle to aid the congression of chromosomes. Because deregulation of mitotic processes leads to chromosomal instability, known as marker of cancer, the importance of clathrin in normal mitosis may be relevant to understanding human cancers. We have previously shown that kinetochore proteins, CENP-A and CENP-H, are upregulated in human primary colon cancer, and their

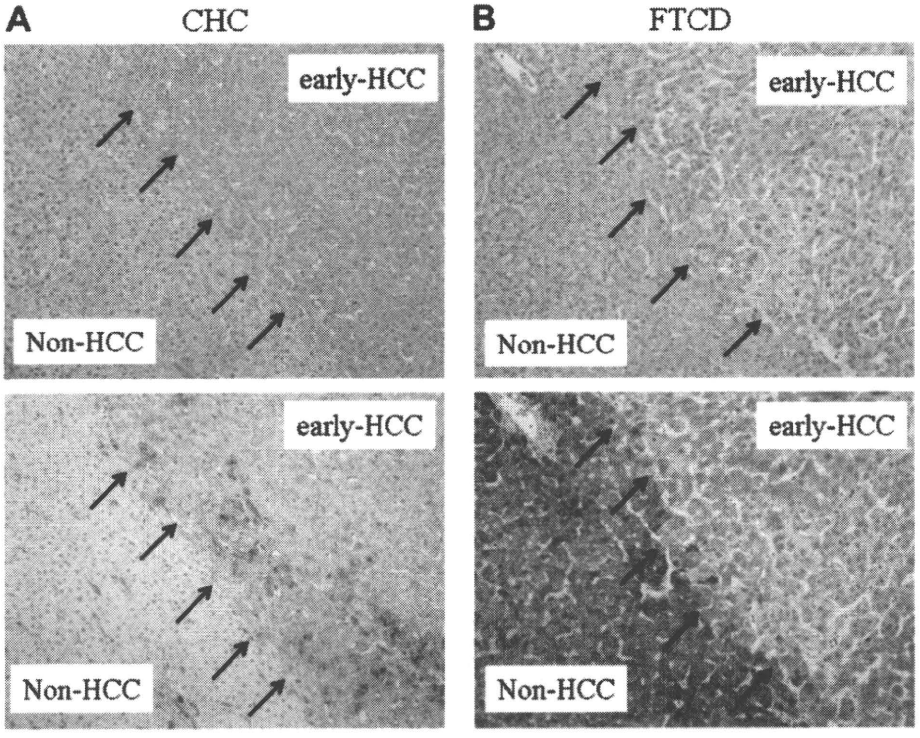

Fig. 5. Immunohistochemical analyses of differential protein expression in early HCC tissues. Early HCC tissues were stained with hematoxylin-eosin (upper panel) or with anti-CHC (clathrin heavy chain)/FTCD (formiminotransferase cyclodeaminase) antibody (lower panel). Arrows indicate borders between early HCC and nontumor tissue. (A) Early HCCs were distinguished from adjacent nontumor tissues by stronger staining of CHC. (B) Early HCCs showed weaker staining of FTCD than adjacent nontumor tissues.

overexpression induces aneuploidy.[14,27] Similarly, the up-regulation of CHC observed in this study might cause chromosome missegregation and lead to HCC development.

FTCD showed strong uniform staining in most nontumor tissue, whereas weak staining was observed in HCC. Interestingly, the intensity of FTCD staining in well-differentiated HCC tissues was more likely to be stronger than that in poorly differentiated HCC tissues, suggesting that the expression of FTCD might be involved in the dedifferentiation of tumor cells. FTCD was previously identified as a 58-kDa rat liver protein with the cytoplasmic surface of the Golgi apparatus *in vivo*.[28] It is considered that FTCD is a liver-specific enzyme that controls folic acid metabolism.[29] Although FTCD has also been recognized as a liver-specific antigen recognized by the sera of patients with autoimmune hepatitis,[30] its involvement in carcinogenesis has not been reported. Thus, our observation is the first report that suggests that down-regulation of FTCD participates in liver carcinogenesis. Further studies are needed to elucidate the precise mechanism of FTCD down-regulation in HCC.

Ku86 is a DNA end-binding molecule that plays an important role in the process of DNA damage signaling and repair, which is thought to maintain genomic stability. Mice deficient in Ku86 showed a marked increase in chromosomal aberrations, and the loss of p53 and Ku86 promotes tumorigenesis, which suggests that Ku86 suppresses tumor development by maintaining the integrity of the genome.[31] Furthermore, recent observation showed that haplo-insufficiency of Ku80 (=Ku86) in poly(ADP-ribose) polymerase-1 (PARP-1)$^{-/-}$ mice promotes the development of hepatocellular adenoma and hepatocellular carcinoma,[32] suggesting that down-regulation of Ku80 is also important for liver carcinogenesis. In contrast, there are some examples in which the up-regulation of Ku86 is associated with tumor progression. Increased expression of Ku70 and Ku86 in a COX-2–dependent mechanism might be associated with hyperproliferation of gastric cancer cells.[33] In addition, increased expression of Ku86 has been reported in B-cell chronic lymphocytic leukemia and in aggressive breast tumors.[34,35] More precise work is needed to examine the expression level of Ku86 in various tumors and to test whether overexpression of Ku86 is a cause or consequence of tumorigenesis.

Rhodanese (EC 2.8.1.1) was originally identified as a mitochondrial matrix enzyme and was proposed to play a role in cyanide detoxification.[36] Recently, it was demonstrated that H_2S is a potent toxin normally present in the colonic lumen, which may play a role in ulcerative colitis, and rhodanese is the principal enzyme involved in H_2S detoxification.[37] In fact, the expression of rhodanese was focally lost in ulcerative colitis.[38] Moreover, rhodanese was markedly reduced in advanced colon cancer.[38] Given that chronic inflammation is an important underlying

condition for tumor development,[39] anti-inflammatory protein such as rhodanese might prevent tumor progression. Recent data have also expanded the concept that inflammation is a critical component of carcinogenesis. In this regard, down-regulation of rhodanese might be a cause of HCC development and could be a potential target for cancer therapy.

Vinculin has a crucial role in the maintenance and regulation of cell adhesion and migration. On recruitment to cell–cell and cell–matrix adherens-type junctions, vinculin becomes activated and mediates various protein–protein interactions that regulate the links between F-actin and the cadherin and integrin families of cell adhesion molecules.[40] Because the loss of cell–cell and cell–matrix interaction is crucial for the development of tumors, down-regulation of vinculin might contribute to carcinogenesis. In fact, the expression of vinculin was repressed in lung carcinoma in surfactant protein C (SP-C)/c-raf transgenic mice.[41] Overexpression of vinculin suppresses tumorigenicity in transformed cells,[42] whereas cancer cells lacking vinculin enhance cell motility and are highly metastatic.[43,44] Our finding that vinculin was repressed in HCC further supports its tumor suppressor function. Interestingly, although full-length vinculin is 117 kDa, smaller molecular weight protein (the major one being 60 kDa) was observed and down-regulated in nontumor tissues. Several reports have shown proteolytic cleavage of vinculin. For example, vinculin is proteolyzed by calpain into at least three fragments (105, 95, 85 kDa[45]) during platelet aggregation. Conversely, alpha-actinin–vinculin interactions causes the conformational change of vinculin and generate an approximately 60-kDa fragment of vinculin by papain treatment[46]; therefore, it is necessary to confirm whether these low molecular proteins are degradation products of vinculin.

In summary, we identified several proteins that are useful to confirm the diagnosis of HCC. They could make significant contributions to the diagnosis of HCC and might also be potential therapeutic targets for cancer control and prevention. Further investigation is needed to uncover the mechanisms responsible for altered protein expressions in HCC.

References

1. Parkin DM, Bray F, Ferlay J, Pisani P. Estimating the world cancer burden: Globocan 2000. Int J Cancer 2001;94:153-156.
2. Feitelson MA, Sun B, Satiroglu Tufan NL, Liu J, Pan J, Lian Z. Genetic mechanisms of hepatocarcinogenesis. Oncogene 2002;21:2593-2604.
3. Pisani P, Parkin DM, Bray F, Ferlay J. Estimates of the worldwide mortality from 25 cancers in 1990. Int J Cancer 1999;83:18-29.
4. Statistics and Information Dept., Minister's Secretariat, Ministry of Health. Vital statistics of Japan 2003. Tokyo, 2003, 66-67.
5. Llovet JM, Burroughs A, Bruix J. Hepatocellular carcinoma. Lancet 2003; 362:1907-1917.
6. Nomura F, Ishijima M, Kuwa K, Tanaka N, Nakai T, Ohnishi K. Serum des-gamma-carboxy prothrombin levels determined by a new generation of sensitive immunoassays in patients with small-sized hepatocellular carcinoma. Am J Gastroenterol 1999;94:650-654.
7. Bruix J, Sherman M. Management of hepatocellular carcinoma. HEPATOLOGY 2005;42:1208-1236.
8. Liang CR, Leow CK, Neo JC, Tan GS, Lo SL, Lim JW, et al. Proteome analysis of human hepatocellular carcinoma tissues by two-dimensional difference gel electrophoresis and mass spectrometry. Proteomics 2005;5: 2258-2271.
9. Lim SO, Park SJ, Kim W, Park SG, Kim HJ, Kim YI, et al. Proteome analysis of hepatocellular carcinoma. Biochem Biophys Res Commun 2002;291:1031-1037.
10. Li C, Hong Y, Tan YX, Zhou H, Ai JH, Li SJ, et al. Accurate qualitative and quantitative proteomic analysis of clinical hepatocellular carcinoma using laser capture microdissection coupled with isotope-coded affinity tag and two-dimensional liquid chromatography mass spectrometry. Mol Cell Proteomics 2004;3:399-409.
11. Santamaria E, Munoz J, Fernandez-Irigoyen J, Prieto J, Corrales FJ. Toward the discovery of new biomarkers of hepatocellular carcinoma by proteomics. Liver Int 2007;27:163-173.
12. Wright LM, Kreikemeier JT, Fimmel CJ. A concise review of serum markers for hepatocellular cancer. Cancer Detect Prev 2007;31:35-44.
13. Oh-Ishi M, Satoh M, Maeda T. Preparative two-dimensional gel electrophoresis with agarose gels in the first dimension for high molecular mass proteins. Electrophoresis 2000;21:1653-1669.
14. Tomonaga T, Matsushita K, Yamaguchi S, Oh-Ishi M, Kodera Y, Maeda T, et al. Identification of altered protein expression and post-translational modifications in primary colorectal cancer by using agarose two-dimensional gel electrophoresis. Clin Cancer Res 2004;10:2007-2014.
15. Nishimori T, Tomonaga T, Matsushita K, Oh-Ishi M, Kodera Y, Maeda T, et al. Proteomic analysis of primary esophageal squamous cell carcinoma reveals downregulation of a cell adhesion protein, periplakin. Proteomics 2006;6:1011-1018.
16. Capurro M, Wanless IR, Sherman M, Deboer G, Shi W, Miyoshi E, et al. Glypican-3: a novel serum and histochemical marker for hepatocellular carcinoma. Gastroenterology 2003;125:89-97.
17. Di Tommaso L, Franchi G, Park YN, Fiamengo B, Destro A, Morenghi E, et al. Diagnostic value of HSP70, glypican 3, and glutamine synthetase in hepatocellular nodules in cirrhosis. HEPATOLOGY 2007;45:725-734.
18. Roncalli M, Roz E, Coggi G, Di Rocco MG, Bossi P, Minola E, et al. The vascular profile of regenerative and dysplastic nodules of the cirrhotic liver: implications for diagnosis and classification. HEPATOLOGY 1999;30:1174-1178.
19. Bosch FX, Ribes J, Diaz M, Cleries R. Primary liver cancer: worldwide incidence and trends. Gastroenterology 2004;127:S5-S16.
20. Stachurski D, Miron PM, Al-Homsi S, Hutchinson L, Lee Harris N, Woda B, et al. Anaplastic lymphoma kinase-positive diffuse large B-cell lymphoma with a complex karyotype and cryptic 3′ ALK gene insertion to chromosome 4 q22–24. Hum Pathol 2007;38:940-945.
21. Argani P, Lui MY, Couturier J, Bouvier R, Fournet JC, Ladanyi M. A novel CLTC-TFE3 gene fusion in pediatric renal adenocarcinoma with t(X;17)(p11.2;q23). Oncogene 2003;22:5374-5378.
22. Chikatsu N, Kojima H, Suzukawa K, Shinagawa A, Nagasawa T, Ozawa H, et al. ALK+, CD30-, CD20- large B-cell lymphoma containing anaplastic lymphoma kinase (ALK) fused to clathrin heavy chain gene (CLTC). Mod Pathol 2003;16:828-832.
23. Ma Z, Hill DA, Collins MH, Morris SW, Sumegi J, Zhou M, et al. Fusion of ALK to the Ran-binding protein 2 (RANBP2) gene in inflammatory myofibroblastic tumor. Genes Chromosomes Cancer 2003;37:98-105.
24. Bridge JA, Kanamori M, Ma Z, Pickering D, Hill DA, Lydiatt W, et al. Fusion of the ALK gene to the clathrin heavy chain gene, CLTC, in inflammatory myofibroblastic tumor. Am J Pathol 2001;159:411-415.
25. Dodge GR, Kovalszky I, McBride OW, Yi HF, Chu ML, Saitta B, et al. Human clathrin heavy chain (CLTC): partial molecular cloning, expression, and mapping of the gene to human chromosome 17q11-qter. Genomics 1991;11:174-178.

26. Royle SJ, Bright NA, Lagnado L. Clathrin is required for the function of the mitotic spindle. Nature 2005;434:1152-1157.
27. Tomonaga T, Matsushita K, Ishibashi M, Nezu M, Shimada H, Ochiai T, et al. Centromere protein H is up-regulated in primary human colorectal cancer and its overexpression induces aneuploidy. Cancer Res 2005;65: 4683-4689.
28. Bloom GS, Brashear TA. A novel 58-kDa protein associates with the Golgi apparatus and microtubules. J Biol Chem 1989;264:16083-16092.
29. Bashour AM, Bloom GS. 58K, a microtubule-binding Golgi protein, is a formiminotransferase cyclodeaminase. J Biol Chem 1998;273:19612-19617.
30. Lapierre P, Hajoui O, Homberg JC, Alvarez F. Formiminotransferase cyclodeaminase is an organ-specific autoantigen recognized by sera of patients with autoimmune hepatitis. Gastroenterology 1999;116:643-649.
31. Difilippantonio MJ, Zhu J, Chen HT, Meffre E, Nussenzweig MC, Max EE, et al. DNA repair protein Ku80 suppresses chromosomal aberrations and malignant transformation. Nature 2000;404:510-514.
32. Tong WM, Cortes U, Hande MP, Ohgaki H, Cavalli LR, Lansdorp PM, et al. Synergistic role of Ku80 and poly(ADP-ribose) polymerase in suppressing chromosomal aberrations and liver cancer formation. Cancer Res 2002;62:6990-6996.
33. Lim JW, Kim H, Kim KH. Expression of Ku70 and Ku80 mediated by NF-kappa B and cyclooxygenase-2 is related to proliferation of human gastric cancer cells. J Biol Chem 2002;277:46093-46100.
34. Klein A, Miera O, Bauer O, Golfier S, Schriever F. Chemosensitivity of B cell chronic lymphocytic leukemia and correlated expression of proteins regulating apoptosis, cell cycle and DNA repair. Leukemia 2000;14:40-46.
35. Pucci S, Mazzarelli P, Rabitti C, Giai M, Gallucci M, Flammia G, et al. Tumor specific modulation of KU70/80 DNA binding activity in breast and bladder human tumor biopsies. Oncogene 2001;20:739-747.
36. Scott EM, Wright RC. Genetic polymorphism of rhodanese from human erythrocytes. Am J Hum Genet 1980;32:112-114.
37. Picton R, Eggo MC, Merrill GA, Langman MJ, Singh S. Mucosal protection against sulphide: importance of the enzyme rhodanese. Gut 2002;50:201-205.
38. Ramasamy S, Singh S, Taniere P, Langman MJ, Eggo MC. Sulfide-detoxifying enzymes in the human colon are decreased in cancer and upregulated in differentiation. Am J Physiol Gastrointest Liver Physiol 2006;291:G288-G296.
39. Coussens LM, Werb Z. Inflammation and cancer. Nature 2002;420:860-867.
40. Bakolitsa C, Cohen DM, Bankston LA, Bobkov AA, Cadwell GW, Jennings L, et al. Structural basis for vinculin activation at sites of cell adhesion. Nature 2004;430:583-586.
41. Rutters H, Zurbig P, Halter R, Borlak J. Towards a lung adenocarcinoma proteome map: studies with SP-C/c-raf transgenic mice. Proteomics 2006; 6:3127-3137.
42. Rodriguez Fernandez JL, Geiger B, Salomon D, Sabanay I, Zoller M, Ben-Ze'ev A. Suppression of tumorigenicity in transformed cells after transfection with vinculin cDNA. J Cell Biol 1992;119:427-438.
43. Raz A, Geiger B. Altered organization of cell-substrate contacts and membrane-associated cytoskeleton in tumor cell variants exhibiting different metastatic capabilities. Cancer Res 1982;42:5183-5190.
44. Coll JL, Ben-Ze'ev A, Ezzell RM, Rodriguez Fernandez JL, Baribault H, Oshima RG, et al. Targeted disruption of vinculin genes in F9 and embryonic stem cells changes cell morphology, adhesion, and locomotion. Proc Natl Acad Sci U S A 1995;92:9161-9165.
45. Serrano K, Devine DV. Vinculin is proteolyzed by calpain during platelet aggregation: 95 kDa cleavage fragment associates with the platelet cytoskeleton. Cell Motil Cytoskeleton 2004;58:242-252.
46. Bois PR, Borgon RA, Vonrhein C, Izard T. Structural dynamics of alpha-actinin-vinculin interactions. Mol Cell Biol 2005;25:6112-6122.

J Gastroenterol 2009; 44:228–235
DOI 10.1007/s00535-008-2304-4

Journal of Gastroenterology

Involvement of hepatoma-derived growth factor in the growth inhibition of hepatocellular carcinoma cells by vitamin K_2

Teruhisa Yamamoto, Hideji Nakamura, Weidong Liu, Ke Cao, Shohei Yoshikawa, Hirayuki Enomoto, Yoshinori Iwata, Noritoshi Koh, Masaki Saito, Hiroyasu Imanishi, Soji Shimomura, Hiroko Iijima, Toshikazu Hada, and Shuhei Nishiguchi

Division of Hepatobiliary and Pancreatic Medicine, Department of Internal Medicine, Hyogo College of Medicine, 1-1 Mukogawa-cho, Nishinomiya, Hyogo 663-8501, Japan

Background. Vitamin K_2 has been reported to suppress the growth of human hepatocellular carcinoma (HCC) in vitro and hepatocarcinogenesis in hepatitis C virus (HCV)-related cirrhosis in vivo. Hepatoma-derived growth factor (HDGF) is a unique nuclear targeting growth factor that is highly expressed in HCC cells and is a possible prognostic factor for patients with HCC. We investigated the regulation of HDGF expression by vitamin K_2. ***Methods.*** Three HCC-derived cell lines, HepG2, HuH-7, and SK-Hep-1, were used. Cell number was determined with the MTT assay. The expression levels of HDGF mRNA and protein were measured by the real-time reverse transcriptase-polymerase chain reaction (PCR) method and ELISA and Western blot analysis, respectively. The HDGF promoter activity was measured by a dual luciferase-reporter assay. ***Results.*** Vitamin K_2 suppressed the growth of the three HCC cell lines in a dose-dependent manner. Vitamin K_2 significantly suppressed the expression of the HDGF protein and mRNA in three cell lines. By a luciferase assay, vitamin K_2 significantly suppressed the promoter activity of the HDGF protein. Based on some luciferase-reporter plasmids containing truncated promoter regions, the possible responsive site of vitamin K_2 seems to reside in the region −1 to −150 bp of the HDGF gene. ***Conclusions.*** These findings suggested that regulation of the HDGF gene expression is one of the crucial mechanisms of vitamin K_2-induced cell growth suppression for HCC.

Key words: HDGF, HCC, vitamin K_2, luciferase assay

Received: February 21, 2008 / Accepted: September 27, 2008
Reprint requests to: H. Nakamura

Introduction

Hepatoma-derived growth factor (HDGF) is a unique nuclear targeting growth factor with heparin affinity that was purified and cloned from a human hepatocellular carcinoma (HCC) cell line.[1–4] HDGF has both oncogenic and angiogenic activity.[5,6] HDGF stimulates the proliferation of HCC cells, in addition to fibroblasts, endothelial cells, vascular smooth muscle cells, and fetal hepatocytes, after translocation to the nucleus by use of the bipartite nuclear localization signals.[1–9] HDGF is highly expressed in several cancers including HCC and is closely related to the aggressive biological potential of cancer cells.[10–16] A downregulation of HDGF by antisense oligonucleotides or siRNA treatment suppresses the proliferation of cancer cells that express HDGF endogenously.[14,17] Recently, a significant correlation has been shown between HDGF expression and the prognosis for the recurrence-free and overall survival in patients with HCC.[18,19] HDGF is considered to play an important role in both hepatocarcinogenesis and cancer progression. If HDGF expression is suppressed by drugs or chemical agents, then the growth of HCC cells should be regulated efficiently. However, the regulation mechanism of HDGF expression has not yet been clarified.

Vitamin K, an essential hydrophobic vitamin, and its derivatives have been shown to inhibit the proliferation of cancer cells including HCC.[20–23] However, the precise mechanism of their growth inhibitory action has not yet been clarified. Vitamin K consists of different forms, vitamin K_1–K_5. Vitamin K_2 (menaquinone) is produced by the intestinal flora and is used as an oral medication for patients with osteoporosis. The in vivo preventive effect of vitamin K_2 on the development of HCC, or the recurrence after treatment of HCC, in patients with HCV-related cirrhosis has been reported.[24,25] Recent in vitro studies have advocated some molecular mechanisms for the growth inhibition by vitamin K_2: a pathway

via protein kinase A activation, induction of the cell cycle-regulating proteins including p21, and reduced expression of the cyclin-dependent kinases.[26-29] However, these mechanisms cannot explain the entire suppressive effects of vitamin K_2 on the proliferation of HCC cells. Other unknown mechanisms have been suggested for the cell proliferation inhibitory effects of vitamin K. The transcriptional regulation of the growth factor genes or growth factor receptor genes by vitamin K_2 has not yet been reported.

In the present study, we investigated the regulation of HDGF expression by vitamin K_2 in HCC cells.

Materials and methods

Materials

Vitamin K_2 (menatetrenone, MK-4) was supplied from Eisai Co. (Tokyo, Japan). The human HCC cell lines HepG2, HuH-7, and SK-Hep-1 were purchased from American Type Culture Collection (ATCC). These cell lines were cultured in Dulbecco's modified Eagle's essential medium (DMEM; Gibco BRL, Grand Island, NY, USA) with 10% fetal bovine serum (FBS), penicillin (100 units/ml), and streptomycin (100 μg/ml) at 37°C in a humidified incubator with 5% CO_2.

Cell proliferation assays

The cells were seeded onto 96-well plates at a density of 2.5×10^3 cells. After a 24-h culture, 100 μl fresh medium containing different concentrations of vitamin K_2 (10, 30, and 100 μM) was added in each well. Vitamin K_2 was dissolved in 99% ethanol at the concentration of 10 mM and then diluted with DMEM to the appropriate concentrations for the experiments. Forty-eight hours later, the culture medium was replaced with fresh medium containing different concentrations of vitamin K_2. The control cells were cultured in DMEM containing the corresponding concentration of ethanol to each dose of the vitamin K_2. After a 4-day culture with vitamin K_2 treatment, the number of viable cells in each well was determined with the 3-(4,5-dimethyl-2-thiazolyl-2,5-diophenyl-2*H*-tetrazolium bromide) (MTT) assay (Roche, Nutley, NJ, USA) according to the manufacturer's instructions.

All experiments were carried out in four wells concurrently, and then were repeated three times.

Western blotting

After a 96-h culture with vitamin K_2, the cells were washed twice with ice-cold phosphate-buffered saline (PBS), lysed, and sonicated in RIPA buffer [1× PBS, 1% Nonidet P-40, 0.5% sodium deoxycholate, 0.1% sodium dodecyl sulfate (SDS), 100 μg/ml phenylmethylsulfonyl fluoride, 45 μg/ml aprotinin, 100 mM sodium orthovanadate]. The supernatant of the homogenate was used for protein determination with a BCA Protein Assay Kit (Pierce, Rockford, IL, USA) and electrophoresis. The samples with 5 μg total protein were electrophoresed on a 12.5% SDS-polyacrylamide gel under reducing conditions and blotted to a polyvinylidene difluoride (PVDF) membrane by electroblotting. The membranes were blotted with the anti-C terminus of the HDGF polyclonal antibody at a dilution of 1:10000, which was generated by the New Zealand White rabbit.[3] The signals were developed with an ABC kit (Vector, Burlingame, CA, USA) and diaminobenzidine.

HDGF-overexpressing HepG2 cells

We constructed *myc*-tagged human HDGF in pEF-BOS plasmids and selected and cloned stable transfectants after transfection to HepG2 as described previously.[3]

HDGF-knock-down SK-Hep-1 cells by shRNA

SuperSilencing shRNA plasmid for human HDGF was purchased from SuperArray Bioscience Corporation (catalog number: KH10419N). SK-Hep-1 was seeded at 1×10^5 cells in 6-well plates with 2 ml 10% FBS-DMEM medium. Next day, 2 μg HDGF-shRNA and the negative control shRNA plasmids were transfected into the cells by 5.0 μl Lipofectamine 2000, according to the protocol from SuperArray. The transfected medium was changed by 10% FBS-DMEM with Geneticin (G418), 1200 mg/l, after 24 h. The G418 media were changed every 3 days. The knock-down expression of HDGF protein was confirmed by Western blot in SK-Hep-1 cells selected by G418 media.

A quantitative reverse transcription-polymerase chain reaction (RT-PCR) analysis of HDGF mRNA levels

HDGF mRNA expression was measured by a quantitative real-time PCR according to the method previously reported.[18] In brief, the total RNA was extracted with the AGPC method using Isogen (Nippongene, Tokyo, Japan); 5 μg deoxyribonuclease I-treated total RNA was used for the reverse transcriptase reaction. An aliquot representing 100 ng input RNA was amplified by using a TaqMan PCR Reagent Kit (Applied Biosystems, Foster City, CA, USA) with the ABI PRISM 7700 sequence Detection System (Applied Biosystems) as follows: 50°C for 2 min, 95°C for 10 min, and 40 cycles at 95°C for 15 s, and 60°C for 1 min. The forward primer 5′-AAGTTTGGCAAGCCCAACA-3′, reverse primer 5′-GGCTCTTCCACACAGCTCTTT-3′, and probe

5′-FAM-AACCCTACTGTCAAGGCTTCCGGCT-TAMRA-3′ were used for HDGF. As an internal control, beta-actin mRNA was used. The RNA extracted from HuH-7 cells was used as a standard. After reverse transcription (RT), standard complementary DNA (cDNA) was serially diluted to obtain five standard solutions for use in the PCR reaction to generate the reference curve. The relative amount of cDNA in each sample was measured by the interpolation of the standard curve, and then the relative ratio of the HDGF/beta-actin expression was calculated for each sample.

Luciferase assay of HDGF promoter activity

Constructs of luciferase-reporter plasmids of the HDGF promoter region. The DNA from the HuH-7 cells was extracted by the Isogen method. Thereafter, the DNA was digested by Tth111 I, purified by phenol/chloroform, and precipitated by ethanol. The HDGF promoter DNA was acquired by a nested PCR. First, 0.5 μg digested and purified DNA was amplified by the forward primer HDGF P5F5 (5′-TACGACATCAGGAGTTCG AAACCA-3′) and the reverse primer HDGF P3R (5′-TGCGCGCTCGTCGAGTTGTTTGT-3′) using a LA TAKARA Taq Kit (RR002A) (Takara, Kyoto, Japan). This PCR product was used as the template of the second amplification. The second PCR was done by series primer pairs designed by DNASIS software using a TAKARA Taq Kit. The DNA amplification was performed in the condition of 94°C for 1 min, 55°C for 1 min, and 72°C for 1 min, for 35 cycles.

Plasmid constructs

The PCR products were purified, polished, and inserted into the pGL3 Basic luciferase-reporter vector predigested by *Sma*I, and transfected into *Escherichia coli* by a PCR Cloning Kit (Stratagene, La Jolla, CA, USA), according to the manufacturer's instructions. The isolated plasmids containing the desired HDGF promoters were verified by *Kpn*I plus *Xho*I digestions and sequenced using the RV Primer 3 from the 5′-end and the GL Primer 2 from the 3′-end.

Luciferase assay of luciferase-reporter plasmids

The HepG2 cells (2×10^5 cells/well) were seeded in a 6-well culture dish (Iwaki, Funabashi, Chiba, Japan) in phenol red-free DMEM containing 5% charcoal-dextran-stripped fetal bovine serum (FBS-CCS). The cells were transfected with 2 μg luciferase-reporter vectors by using a Fugene 6 transfection reagent kit (Roche), according to the manufacturer's recommendations. Twenty-four hours later, the culture media were changed to the fresh media with several concentrations (0, 10, 30, and 100 μM) of vitamin K_2. After incubation for 24 h, the cells were harvested and lysed with luciferase lysis buffer (Promega, Madison, WI, USA). The proteins were measured by a BCA protein assay kit. The luciferase activity of each sample was measured by a luciferase assay kit (Promega). The level of induction was calculated by dividing the mean luciferase activity of the samples treated with vitamin K_2 by the mean activity of the untreated control samples. All experiments were carried out in triplicate and repeated at least three times.

Enzyme-linked immunosorbent assay (ELISA) of HDGF protein

The cells were lysed with the RIPA buffer, as described above. After centrifugation at 10000 rpm for 30 min, the supernatants of the cell lysate were used for the measurement of the HDGF protein by an ELISA. An ELISA for the HDGF was developed by the sandwich method using a monoclonal antibody and a polyclonal antibody against HDGF.

Statistical analysis

The results are expressed as the means ± SE. At least three separate experiments were performed for each data point. The statistical analyses were done using Student's unpaired *t* test (two tailed).

Results

Effect of vitamin K_2 on HCC cells

In patients whom vitamin K_2 are administered at clinically used doses, the serum concentration is calculated to reach to about 30 μM. Thus, we used three doses—10, 30, and 100 μM—of vitamin K_2 in the subsequent experiments. Vitamin K_2 suppressed the proliferation of three HCC cell lines in a dose-dependent manner. The inhibitory effects by vitamin K_2 after 96 h treatment at 30 μM and 100 μM are shown for the three HCC cell lines in Fig. 1.

HDGF was expressed in three cell lines (Fig. 2a). The intracellular HDGF amounts in these cell lines were measured by an ELISA (Fig. 2b). HCC cells with higher production of the HDGF protein seem to show higher inhibition of HCC cell proliferation by vitamin K_2, although not significantly. Some growth factors are involved in the proliferation of HCC cells. Next, we knocked down the HDGF expression and assessed its participating level on the proliferation of HCC cells. We obtained two stable HDGF-knock-down clones after transfection of HDGF-shRNA into SK-Hep-1 cells. In

two SK-Hep-1 clones, of which HDGF expressions were stably knock-downed 64% and 40%, their proliferation was significantly suppressed, but partially at about 35% and 11%, in clone 1 (HDGF-shRNA1) and clone 3 (HDGF-shRNA3), respectively (Fig. 2c). Thus, HDGF is partly involved in the proliferation of HCC cells.

Effect of vitamin K_2 on HDGF protein expression in HCC cells

HDGF protein in the HuH-7 cells decreased after vitamin K_2 treatment by a Western blot analysis (data not shown). By the use of an ELISA for HDGF, we measured intracellular levels of HDGF protein in three HCC cell lines after vitamin K_2 treatment for 96 h. The vitamin K_2 treatment significantly suppressed the HDGF protein expression on three HCC cell lines (Fig. 3).

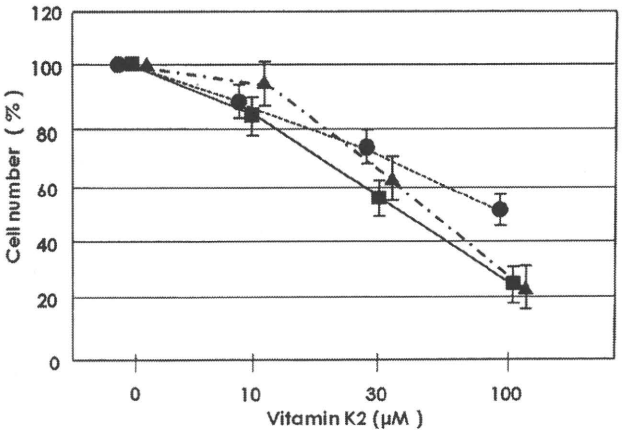

Fig. 1. Vitamin K_2 suppressed the proliferation of human hepatocellular cells dose-dependently. HepG2 (●), HuH-7 (▲), and SK-Hep-1 (■) were treated with various concentrations of vitamin K_2. After vitamin K_2 treatment for 96 h, the cell numbers were determined by the MTT method. Data are mean ± SE of three independent experiments

Recovery of vitamin K_2-induced suppression of HCC proliferation by overexpression of HDGF

Next, we investigated the restorative effect of HDGF on the suppression of HCC cell proliferation by vitamin K_2 by use of HDGF-overexpressing HepG2 cells. The overexpression of HDGF significantly recovered the vitamin K_2-induced suppression of HepG2 cell proliferation, but partially, about 50% (Fig. 4). Thus, these findings suggest that the suppression of HDGF expression is one pathway of vitamin K_2-mediated growth inhibitory mechanisms in HCC cells.

Effect of vitamin K_2 on HDGF mRNA expression

HDGF mRNA expression was measured by a quantitative real-time PCR method. In the HepG2, HuH-7, and SK-Hep-1 cells, HDGF mRNA expression was suppressed 36.5%, 39.5%, and 22.5%, respectively, after vitamin K_2 treatment for 96 h at the dose of 30 μM. The HDGF mRNA expression was suppressed by vitamin K_2 at 51.1%, 63.3%, and 66.2% in the HepG2, HuH-7, and SK-Hep-1 cells, respectively, at the dose of 100 μM (Fig. 5). Next, we investigated whether vitamin K_2 suppressed the promoter activity of HDGF by a dual luciferase assay. It is difficult to transfect plasmids to HuH-7 cells, and we examined this reporter assay in the other two HCC cell lines. In the HepG2 and SK-Hep-1 cells, vitamin K_2 significantly suppressed the luciferase

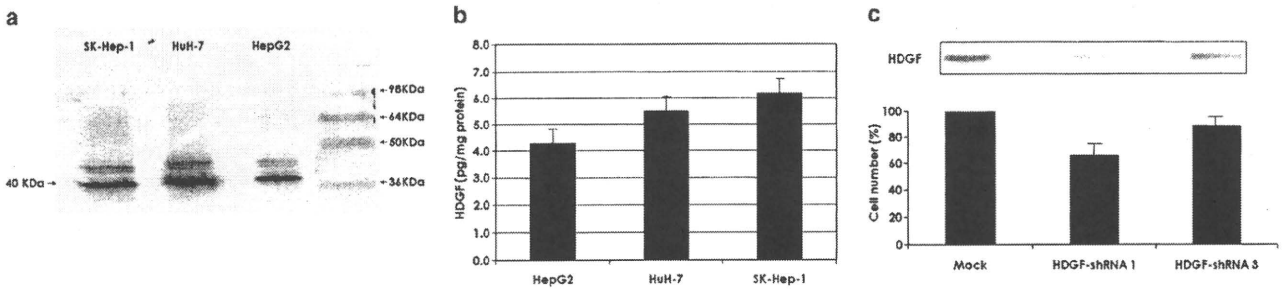

Fig. 2. Expression of hepatoma-derived growth factor (HDGF) protein in human HCC cell lines. Three HCC cell lines were lysed and vortexed with lysis buffer after 48 h culture. After centrifugation, the supernatants of each cell line were used for analysis. **a** Western blot analysis. The cell lysate with 5 μg protein from each cell line was loaded and electrophoresed. After electroblotting, the membrane was blotted with anti-HDGF antibody (C-terminus) at a dilution of 1:10000. **b** Intracellular HDGF protein by an enzyme-linked immunosorbent assay (ELISA). The cell lysates after centrifugation were analyzed in an ELISA kit for HDGF. Data are mean ± SE of three independent experiments. **c** Knock-down of HDGF expression suppressed the proliferation of SK-Hep-1 cells. The stably HDGF-knock-down SK-Hep-1 clones (HDGF-shRNA1 and -3) and mock cells were cultured for 96 h, and then cell numbers were measured by MTT assay. HDGF protein expression in each clone was shown by Western blot

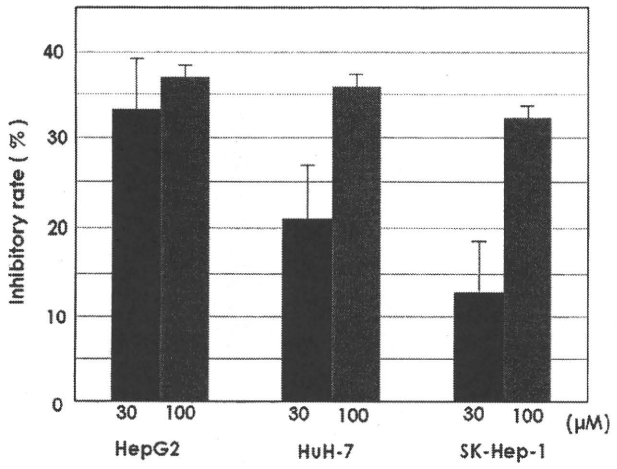

Fig. 3. HDGF protein expression in HCC cells was suppressed by vitamin K_2. Inhibitory rate of HDGF protein expression by vitamin K_2 is shown. Three HCC cell lines were treated with vitamin K_2 at the dose of 30 μM or 100 μM for 96 h. The HCC cells were lysed and vortexed with lysis buffer, and the cell lysates after centrifugation were analyzed by an ELISA kit for HDGF. The data are shown as the mean ± SE of three independent experiments

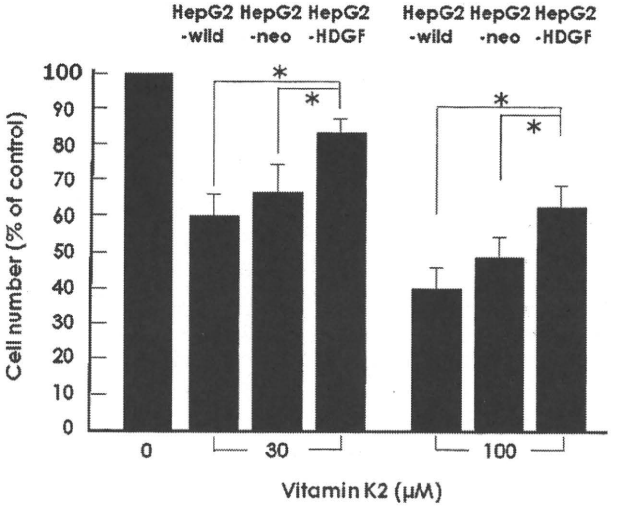

Fig. 4. HDGF overexpression recovered the vitamin K_2-induced suppression of cell proliferation. HDGF-overexpressing HepG2 (HepG2-HDGF), mock (HepG2-neo), and parent HepG2 (HepG2-wild) cells were treated with 30 or 100 μM vitamin K_2. Ninety-six hours later, cell numbers of each well were measured by MTT assay. $*P < 0.05$

activity by 47.7% and 86.9%, respectively, at 30 μM vitamin K_2 after transfection of the H2 promoter (Fig. 6). The luciferase activity was suppressed 78.2% and 97.0% in the HepG2 and SK-Hep-1 cells at the dose of 100 μM, respectively. Therefore, vitamin K_2 significantly suppressed the gene expression of HDGF in the HCC cells.

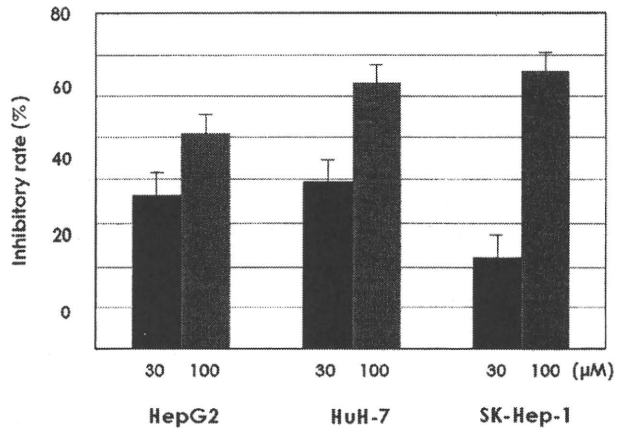

Fig. 5. HDGF mRNA expression was suppressed by vitamin K_2. Three HCC cell lines were treated with vitamin K_2 at 30 μM or 100 μM for 96 h. After RNA extraction, HDGF mRNA expression was measured by the quantitative real-time PCR method. The data are shown as the mean ± SE of three independent experiments

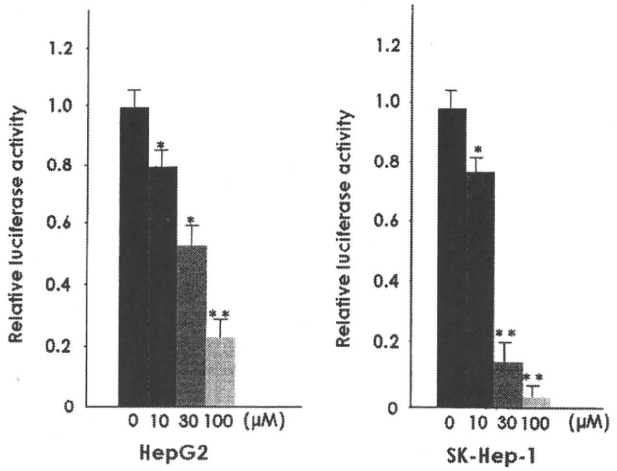

Fig. 6. Vitamin K_2 suppressed the transcription of HDGF. HepG2 and SK-Hep-1 were transfected with 1 μg promoter vector (pLuc-H2). After incubation with the indicated concentrations (μM) of vitamin K_2 for 24 h, the cells were harvested and the relative luciferase activities were measured. The data are shown as the mean ± SE of three independent experiments. $*P < 0.05$; $**P < 0.01$ vs. control

Possible interaction site of vitamin K_2 in the promoter of the HDGF gene

Next, we constructed the luciferase-reporter plasmids including a truncated promoter region (Fig. 7a). The luciferase activity of the H2 promoter was significantly suppressed in the SK-Hep-1 cells, but that of H12 or -13 was not (Fig. 7b). Therefore, the interaction site of vitamin K_2 seems to reside in the region −1 to −150 bp of the HDGF gene. These findings suggest that the sup-

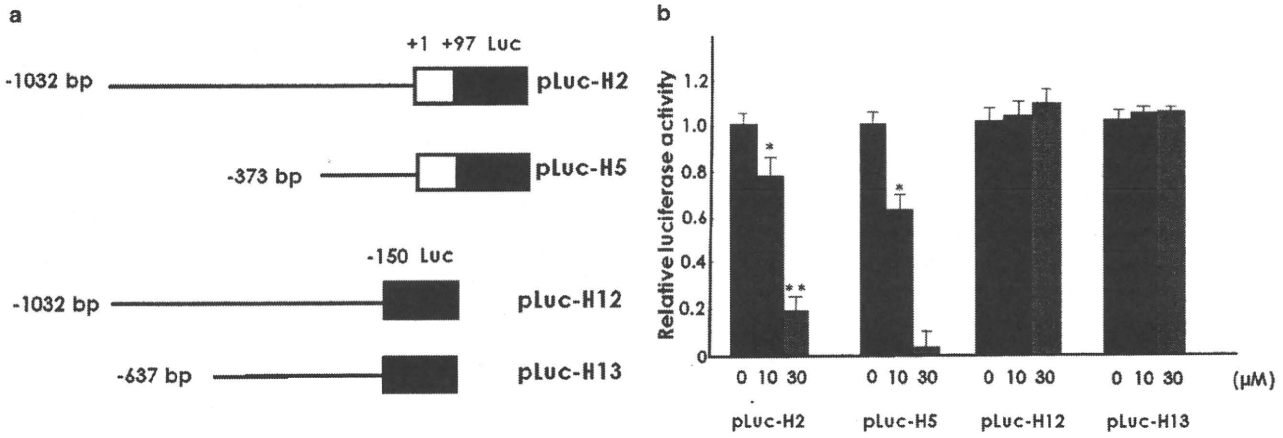

Fig. 7. Possible action site of vitamin K_2 in the promoter of the HDGF gene. **a** The construct of the luciferase-reporter assay plasmids for the HDGF promoter region. **b** SK-Hep-1 cell was transfected with 1 μg each promoter vector (pLuc-H2, -H5, -H12, -H13). After incubation with the indicated concentrations (μM) of vitamin K_2 for 24 h, the cells were harvested, and the relative luciferase activities were measured. Data are shown as mean ± SE of three independent experiments. $^*P < 0.05$; $^{**}P < 0.01$ vs. control

pression of HDGF is one of the pathways to inhibit cell growth by vitamin K_2 treatment, through its interaction with the promoter region of the HDGF gene.

Discussion

The inhibitory mechanisms of vitamin K_2 in cancer cell proliferation have not yet been clarified. Some possible pathways of vitamin K_2 action have been reported, specifically protein kinase A activation, the induction of cell-cycle regulatory proteins, and the suppression of the cyclin-dependent kinases.[26–28] Another pathway has been reported to suppress the cyclin D1 expression through the inhibition of nuclear factor (NF) kappa B activation.[29] Recently, vitamin K_2 is reported to inhibit the phosphorylation of the retinoid X receptor (RXR) alpha protein, which is a critical factor for hepatocarcinogenesis.[30] We previously reported that p21 induction is a significantly important pathway for the growth inhibitory action of vitamin K_2 by the use of HepG2 cells.[28] However, vitamin K_2 suppressed the growth of the HuH-7 cells more strongly than the HepG2 cells, although the HuH-7 cells are deficient in the p21WAF1/CIP1 protein. Therefore, other mechanisms for the vitamin K_2 growth inhibition remained to be clarified.

In the present study, vitamin K_2 significantly suppressed HDGF mRNA and protein expression in HCC cells. Few data have been reported about the inhibition of the expression of growth factor and/or growth factor receptor genes in HCC cells. Acyclic retinoid suppressed fibroblast growth factor (FGF) receptor 3 gene expression in an HCC cell line.[31] Therefore the downregulation of HDGF by vitamin K_2 should play an important role in the suppression of HCC cell growth by vitamin K_2.

HDGF is one of the critical growth factors that play important roles in the proliferation of HCC cells. Enhanced expression of HDGF showed malignant potential of tumor cells and a poorer prognosis in patients with HCC as well as gastric cancer, lung cancer, and pancreatic cancer.[12,13,15,16,18,19,32] Downregulation of HDGF may induce cancer growth inhibition and improve the prognosis for cancer patients. Indeed, the downregulation of HDGF by either antisense oligonucleotides or antisense viral treatment and gene silencing by siRNA inhibit the cell growth both in vitro and in vivo.[8,14,17] In the present study, the knock-down expression of HDGF by shRNA partially suppressed the proliferation of SK-Hep-1 cells. Thus, HDGF is apparently one of the growth factors involved in the proliferation of HCC cells. On the other hand, other growth factors, including hepatocyte growth factor (HGF), FGF, epidermal growth factor (EGF), HB-EGF, and transforming growth factor-alpha (TGF-α), should be related to the proliferation of HCC; however, until now, no evidence has been reported that vitamin K_2 suppressed these growth factors and their receptors. In the present study, we showed a significant suppression of the HDGF gene expression by vitamin K_2. This is the first report that vitamin K_2 regulates the expression of growth factor genes. The regulation of the gene expression of one growth factor, HDGF, by vitamin K_2 suggests to us an important approach to investigate the mechanisms of vitamin K action.

By a luciferase assay using the promoter region of HDGF, vitamin K_2 significantly downregulated the

HDGF expression. Vitamin K_2 must act directly or indirectly on the promoter region of HDGF and regulate the expression of HDGF. Recently, vitamin K_2 suppressed cyclin D1 expression through inhibition of nuclear factor (NF)-kappaB activation with inhibition of phosphorylation and degradation of I-kappaB alpha and I-kappaB kinase activity.[29] In the promoter region of −150 to 0 in the HDGF gene, no NF-kappaB binding site could be detected. Other transcriptional factors, including cAMP response element-binding protein (CREB), upstream transcription factor (USF), and activating enhancer-binding protein (AP)-2, are reported to mediate the vitamin K_2 effects; however, their binding motifs are absent in this promoter region of HDGF (−1 to −150). Therefore, another pathway should be critical for the suppression of the HDGF gene expression by vitamin K_2. It remains to be clarified whether vitamin K_2 directly reacts to the DNA sequence or indirectly via other factors, including transcriptional regulatory factors or binding cofactors. Vitamin K_2 may possibly downregulate some of other growth factor genes, too. It is very important to clarify the mechanism whereby vitamin K_2 reacts on and suppresses the promoter activity of the HDGF gene. These findings suggested that the regulation of growth factor gene expression is one of the crucial mechanisms of the vitamin K_2-induced cell growth inhibition.

In conclusion, the downregulation of the HDGF expression in the promoter region is one of the growth inhibitory mechanisms of vitamin K_2. To elucidate the suppressive mechanism of the HDGF promoter region by vitamin K_2 will possibly lead to the development of a novel growth inhibitory mechanism, thus resulting in a new drug design.

Acknowledgments. This study was supported by a Grant-in-aid of Hyogo Science and Technology Association, Grant-in-aid for researchers, Hyogo College of Medicine, and Health and Labour Sciences Research Grants (Research on Hepatitis).

References

1. Nakamura H, Kambe H, Egawa T, Kimura Y, Ito H, Hayashi E, et al. Partial purification and characterization of hepatoma-derived growth factor. Clin Chim Acta 1989;183:273–84.
2. Nakamura H, Izumoto Y, Kambe H, Kuroda T, Mori T, Kawamura K, et al. Molecular cloning of complementary DNA for a novel human hepatoma-derived growth factor. J Biol Chem 1994;269: 25143–9.
3. Kishima Y, Yamamoto H, Izumoto Y, Yoshida K, Enomoto H, Yamamoto M, et al. Hepatoma-derived growth factor stimulates cell growth after translocation to the nucleus by nuclear localization signals. J Biol Chem 2002;277:10315–22.
4. Everett AD, Stoops T, McNamara CA. Nuclear targeting is required for hepatoma-derived growth factor-stimulated mitogenesis in vascular smooth muscle cells. J Biol Chem 2001;276: 37564–8.
5. Okuda Y, Nakamura H, Yoshida K, Enomoto H, Uyama H, Hirotani T, et al. Hepatoma-derived growth factor induces tumorigenesis in vivo through both direct angiogenic activity and induction of vascular endothelial growth factor. Cancer Sci 2003;94:1034–1041.
6. Everett AD, Narron JV, Stoops T, Nakamura H, Tucker A. Hepatoma-derived growth factor is a pulmonary endothelial cell-expressed angiogenic factor. Am J Physiol Lung Cell Mol Physiol 2004;286:L1194–201.
7. Oliver JA, Al-Awqati Q. An endothelial growth factor involved in rat renal development. J Clin Invest 1998;102:1208–19.
8. Enomoto H, Yoshida K, Kishima Y, Kinoshita T, Yamamoto M, Everett AD, et al. Hepatoma-derived growth factor is highly expressed in developing liver and promotes fetal hepatocyte proliferation. Hepatology 2002;36:1519–27.
9. Everett AD, Lobe DR, Matsumura ME, Nakamura H, McNamara CA. Hepatoma-derived growth factor stimulates smooth muscle cell growth and is expressed in vascular development. J Clin Invest 2000;105:567–75.
10. Yoshida K, Nakamura H, Okuda Y, Enomoto H, Kishima Y, Uyama H, et al. Expression of hepatoma-derived growth factor in hepatocarcinogenesis. J Gastroenterol Hepatol 2003;18:1293–301.
11. Huang JS, Chao CC, Su TL, Yeh SH, Chen DS, Chen CT, et al. Diverse cellular transformation capability of overexpressed genes in human hepatocellular carcinoma. Biochem Biophys Res Commun 2004;315:950–8.
12. Iwasaki T, Nakagawa K, Nakamura H, Takada T, Matsui K, Kawahara K. Hepatoma-derived growth factor as a prognostic marker in completely resected non-small-cell lung cancer. Oncol Rep 2005;13:1075–80.
13. Uyama H, Tomita Y, Nakamura H, Nakamori S, Zhang B, Hoshida Y, et al. Hepatoma-derived growth factor is a novel prognostic factor for patients with pancreatic cancer. Clin Cancer Res 2006;12:6043–8.
14. Zhang J, Ren H, Yuan P, Lang W, Zhang L, Mao L. Downregulation of hepatoma-derived growth factor inhibits anchorage-independent growth and invasion of non-small cell lung cancer cells. Cancer Res 2006;66:18–23.
15. Yamamoto S, Tomita Y, Hoshida Y, Takiguchi S, Fujiwara Y, Yasuda T, et al. Expression of hepatoma-derived growth factor is correlated with lymph node metastasis and prognosis of gastric carcinoma. Clin Cancer Res 2006;12:117–22.
16. Yamamoto S, Tomita Y, Hoshida Y, Morii E, Yasuda T, Doki Y, et al. Expression level of hepatoma-derived growth factor correlates with tumor recurrence of esophageal carcinoma. Ann Surg Oncol 2007;14:2141–9.
17. Kishima Y, Yoshida K, Enomoto H, Yamamoto M, Kuroda T, Okuda Y, et al. Antisense oligonucleotides of hepatoma-derived growth factor (HDGF) suppress the proliferation of hepatoma cells. Hepatogastroenterology 2002;49:1639–44.
18. Yoshida K, Tomita T, Okuda Y, Yamamoto S, Enomoto H, Uyama H, et al. Hepatoma-derived growth factor is a novel prognostic factor for hepatocellular carcinoma. Ann Surg Oncol 2006;13:159–67.
19. Hu TH, Huang CC, Liu LF, Lin SY, Chang HW, Changchien CS, et al. Expression of hepatoma-derived growth factor in hepatocellular carcinoma. Cancer (Phila) 2003;98:1444–56.
20. Chlebowski RT, Akman SA, Block JB. Vitamin K in the treatment of cancer. Cancer Treat Rev 1985;12(1):49–63.
21. Wang Z, Wang M, Finn F, Carr BI. The growth inhibitory effects of vitamins K and their actions on gene expression. Hepatology 1995;22:876–82.
22. Hitomi M, Nonomura T, Yokoyama F, Yoshiji H, Ogawa M, Nakai S, et al. In vitro and in vivo antitumor effects of vitamin K5 on hepatocellular carcinoma. Int J Oncol 2005;26:1337–44.
23. Hitomi M, Yokoyama F, Kita Y, Nonomura T, Masaki T, Yoshiji H, et al. Antitumor effects of vitamins K_1, K_2 and K_3 on hepatocellular carcinoma in vitro and in vivo. Int J Oncol 2005;26:713–20.

24. Habu D, Shiomi S, Tamori A, Takeda T, Tanaka T, Kubo S, et al. Role of vitamin K_2 in the development of hepatocellular carcinoma in women with viral cirrhosis of the liver. JAMA 2004; 292:358–61.
25. Mizuta T, Ozaki I, Eguchi Y, Yasutake T, Kawazoe S, Fujimoto K, et al. The effect of menatetrenone, a vitamin K_2 analog, on disease recurrence and survival in patients with hepatocellular carcinoma after curative treatment: a pilot study. Cancer (Phila) 2006;106:867–72.
26. Markovits J, Wang Z, Carr BI, Sun TP, Mintz P, Le Bret M, et al. Differential effects of two growth inhibitory K vitamin analogs on cell cycle regulating proteins in human hepatoma cells. Life Sci 2003;72:2769–84.
27. Otsuka M, Kato N, Shao RX, Hoshida Y, Ijichi H, Koike Y, et al. Vitamin K_2 inhibits the growth and invasiveness of hepatocellular carcinoma cells via protein kinase A activation. Hepatology 2004;40:243–51.
28. Liu W, Nakamura H, Yamamoto T, Ikeda N, Saito M, Ohno M, et al. Vitamin K_2 inhibits the proliferation of HepG2 cells by up-regulating the transcription of p21 gene. Hepatol Res 2007;37: 360–5.
29. Ozaki I, Zhang H, Mizuta T, Ide Y, Eguchi Y, Yasutake T, et al. Menatetrenone, a vitamin K_2 analogue, inhibits hepatocellular carcinoma cell growth by suppressing cyclin D1 expression through inhibition of nuclear factor kappaB activation. Clin Cancer Res 2007;13:2236–45.
30. Kanamori T, Shimizu M, Okuno M, Matsushima-Nishiwaki R, Tsurumi H, Kojima S, et al. Synergistic growth inhibition by acyclic retinoid and vitamin K_2 in human hepatocellular carcinoma cells. Cancer Sci 2007;98:431–7.
31. Shao RX, Otsuka M, Kato N, Taniguchi H, Hoshida Y, Moriyama M, et al. Acyclic retinoid inhibits human hepatoma cell growth by suppressing fibroblast growth factor-mediated signaling pathways. Gastroenterology 2005;128:228–31.
32. Ren H, Tang X, Lee JJ, Feng L, Everett AD, Hong WK, et al. Expression of hepatoma-derived growth factor is a strong prognostic predictor for patients with early-stage non-small cell lung cancer. J Clin Oncol 2004;22:3230–7.

Bmi-1 gene is upregulated in early-stage hepatocellular carcinoma and correlates with ATP-binding cassette transporter B1 expression

Kathryn Effendi,[1,3] Taisuke Mori,[1,3] Mina Komuta,[1] Yohei Masugi,[1] Wenlin Du[1] and Michiie Sakamoto[1,2]

[1]Department of Pathology, School of Medicine, Keio University, Tokyo, Japan

(Received September 29, 2009/Revised October 24, 2009/Accepted November 1, 2009/Online publication January 19, 2010)

Overexpression of "stemness gene" *Bmi-1* has been identified in some solid tumors. We investigated *Bmi-1* expression in hepatocellular carcinoma (HCC) and ATP-binding cassette transporter B1 (*ABCB1*) as a new potential target for *Bmi-1*. *Bmi-1* was highly expressed in HCC cell lines and the most well differentiated cell line, KIM-1, showed the highest expression. Immunohistochemical, immunocytochemical, and immunoelectron microscopic analysis showed the Bmi-1 protein as having a high intensity of small dots within the nucleus which reflected concentrated sites of Bmi-1 repressive activity. Clear "dot-pattern" staining was observed in 24 of 37 (65%) well differentiated HCC (including 13 of 21 early nodules [62%]), in 32 of 71 (45%) moderately differentiated HCC, and 7 of 14 (50%) poorly differentiated HCC. A similar expression was not observed in non-cancerous background regions. High Bmi-1 expression was observed in the early and well differentiated HCC. Furthermore, overexpression and suppression of *Bmi-1* was followed by a respective increase and decrease in *ABCB1* expression. As with *Bmi-1*, high *ABCB1* expression was also observed in the early and well differentiated HCC. A strong correlation between *ABCB1* and *Bmi-1* mRNA expression was seen in HCC cell lines and clinical samples (Pearson's correlation coefficient 0.95 and 0.90, respectively). The *Bmi-1* gene is upregulated in HCC, and in particular is highly expressed in early and well differentiated HCC. The fact that this expression correlated with that of *ABCB1* suggests a new regulation target for *Bmi-1*, and gives new insight into early hepatocarcinogenesis mechanisms and potential targets for future HCC treatment. (*Cancer Sci* 2010; 101: 666–672)

Hepatocellular carcinoma (HCC) is the sixth most common malignancy in the world and still ranks as the third highest cause of cancer-related death globally.[1] Although individual risks for hepatocarcinogenesis, such as hepatitis viral infection, excessive alcohol intake, and non-alcoholic steatohepatitis are well established, a poor prognosis of HCC is still unavoidable due to the unclear mechanism of hepatocarcinogenesis. HCC is characterized by a multistage process of tumor progression,[2] and molecular changes, particularly in the early stage of HCC, have rarely been shown. The idea of using stem cell principles to understand tumor development and progression has emerged because they share similar characteristics. Recent reports on cancer stem cells or acquirement of stem cell-like properties in various tumors have greatly increased the possible connection of these cells in tumorigenesis.[3,4] *Bmi-1* was first identified as a proto-oncogene that cooperates with c-*myc* to generate mouse pre-B cell lymphomas.[5] Some reports show that *Bmi-1* might induce immortalization by regulating human telomerase reverse transcriptase (hTERT) expression,[6–9] and might play a role in tumorigenesis by acting as a negative regulator of the INK4a/ARF locus that encodes two important tumor suppressors in human cancer, *p16* and *p19*.[10,11] The overexpression of *Bmi-1* has been identified in lymphoma[12,13] and in a few solid tumors such as lung, colorectal, nasopharyngeal, bladder, and HCC.[9,14–18] Many reports mainly focus on *Bmi-1* expression in the advanced stages of cancer and its role in a poor prognosis. However, the exact mechanistic role of *Bmi-1* in tumorigenesis is not clear. In HCC, inactivation of *p16* expression, a well-known target of *Bmi-1*, is already observed in the early stages of hepatocarcinogenesis, due to methylation or an epigenetic mechanism.[19,20] This suggests that another target in the *Bmi-1* signaling pathway should exist. Therefore, we examined the involvement of the "stemness gene" *Bmi-1* and its new potential downstream target in hepatocarcinogenesis.

To our knowledge, there are no studies clearly showing a subcellular expression pattern of *Bmi-1* as a high intensity of small dots within the nucleus in cancer cells. Herein, we examined the expression patterns of *Bmi-1* in HCC cell lines and clinical specimens by immunohistochemistry, and these were confirmed with immunocytochemistry and immunoelectron microscopy. We also examined the expression levels of the ATP-binding cassette transporter B1 (*ABCB1*), listed as one of the genes upregulated after *Bmi-1* induction in bone marrow stromal cells.[6] We hypothesize the potential for *ABCB1* to be a new target for *Bmi-1*. Immunohistochemical staining and mRNA expression level of *ABCB1* were analyzed to investigate the correlation between *Bmi-1* and *ABCB1*.

Materials and Methods

Cell culture. The human HCC cell lines, PLC/PRF/5 and HepG2, were obtained from the American Type Culture Collection (Manassas, VA, USA). KIM-1, KYN-2, and Li7 were established as reported previously.[21] All the cells were grown in RPMI-1640 medium supplemented with 10% FBS, 100 U/mL penicillin, and 100 μg/mL streptomycin.

Tissue specimens of HCC. HCCs and corresponding non-cancerous liver tissue were obtained from 100 patients with 122 nodules (37 well differentiated [including 21 early], 71 moderately differentiated, and 14 poorly differentiated HCCs) who underwent surgical resection at Keio University Hospital (Tokyo, Japan) between 2003 and 2006. The specimens were fixed in 10% formalin and embedded in paraffin. Three pathologists evaluated the histological diagnosis according to the criteria set by the World Health Organization.[22] The histological grade for HCC where different types were found within the same nodule was determined by the predominant histological grade. Primary hepatocytes were harvested from the autopsy of a human fetal liver donor with signed, informed consent. The cells were resuspended in growth medium (10% FBS in DMEM, containing 0.1 mM non-essential amino acid and 0.1 mM sodium pyruvate solution; Gibco BRL, Grand Island, NY,

[2]To whom correspondence should be addressed.
E-mail: msakamot@sc.itc.keio.ac.jp
[3]These authors contributed equally to this work.

doi: 10.1111/j.1349-7006.2009.01431.x

USA), and were maintained at 37°C in a humidified atmosphere containing 95% air and 5% CO_2. This study was carried out with the approval of the Ethics Committee of Keio University School of Medicine.

Real-time quantitative RT-PCR. Real-time quantitative RT-PCR (qRT-PCR) analysis was carried out as previously reported,[6] at least three times, including a no-template negative control. A total of 15 (five well differentiated, seven moderately differentiated, and three poorly differentiated) HCC clinical samples were used. The primer sets were: *Bmi-1* forward, 5′-GAGGGTACTTCATTGATGCCACAAC-3′ and reverse, 5′-GCTGGTCTCCAGGTAACGAACAATA-3′; *ABCB1* forward, 5′-GAGGCCAACATACATGCCTTCA-3′ and reverse, 5′-GGC TGTCTAACAAGGGCACGA-3′.

Immunohistochemical and immunocytochemical analysis. Immunohistochemical staining was done on formalin-fixed, paraffin-embedded tissue sections. These were heated at 120°C in 0.01 mol/L sodium citrate buffer, pH 7.0, for 10 min before incubation with a mouse Bmi-1 antibody (1/200; Upstate Biotechnology, Lake Placid, NY, USA) and a multidrug resistance protein 1 (MDR1) antibody (1/200; Santa Cruz Biotechnology, Santa Cruz, CA, USA). Sections were then incubated with ImmPRESS antimouse Ig kit secondary antibody (Vector Laboratories, Burlingame, CA, USA), and stained with diaminobenzidine. For immunocytochemical analysis, KIM-1 cells were grown to confluence on glass slides, fixed, and washed. The slides were incubated with the Bmi-1 antibody (1/200) in PBS containing 1% BSA, followed by FITC-conjugated, antimouse Ig (1/400; Dako, Glostrup, Denmark). Staining was evaluated using the LSM 510 Meta confocal microscope (Carl Zeiss, Oberkochen, Germany). All staining analysis was done at least twice. We defined Bmi-1 staining criteria as follows: distributed diffusely with clear staining of the "dot-pattern" was scored 2+; distributed focally with weak staining of the dot-pattern was scored 1+; and an absence of the dot-pattern was considered negative. Evaluation criteria for ABCB1 were defined as follows: clear staining of irregular canalicular with cytoplasmic staining scored 2+; an irregular canalicular staining pattern scored 1+; and no staining was considered negative.

Immunoelectron microscopy. KIM-1 cells grown to confluence on glass slides were fixed in 4% formaldehyde and incubated overnight at 4°C with the Bmi-1 antibody (1/200). After rinsing they were treated with a mouse secondary antibody (1/100; Dako) for 3 h at room temperature, then re-fixed in 1% glutaraldehyde for 10 min. After further rinsing, the sections were stained with diaminobenzidine and post-fixed in 2% osmium tetroxide. The slides were dehydrated in graded alcohol, embedded in epoxy resin, and hardened at 60°C for 72 h. Ultrathin sections were cut with an ultramicrotome, stained with uranyl acetate and viewed under a JEOL 1200 EXII transmission electron microscope (Nihon Denshi, Tokyo, Japan).

Immunoblotting. PLC/PRF/5, HepG2, KIM-1, KYN-2, and Li7 cells were lysed in lysis buffer (50 mM Tris-HCL [pH 7.5], 150 mM NaCl, 5 mM EDTA, 1% NP-40, and complete protease inhibitors). Supernatants of the homogenates were subjected to NuPAGE (4–12% Bis-Tris gel; Invitrogen, Carlsbad, CA, USA) by electrophoresis, and transferred to PVDF membranes. Anti-Bmi-1 (1/500), anti-MDR1 (1/200), and anti-actin (1/1000; Sigma, St Louis, MO, USA) were hybridized to the membranes and detected with ECL Western blotting detection reagents (GE Healthcare, Amersham, UK).

Transfection-induced overexpression and RNA interference. Human Bmi-1 full coding cDNA was cloned from the KIM-1 cell line with RT-PCR and inserted into pcDNA53 (Invitrogen). This vector was transfected into the primary fetal hepatocytes using Lipofectamine LTX and positive expression vector-transfected cells were selected with G418 (Invitrogen), according to the manufacturer's instructions. For RNA interference, all purified and pre-annealed siRNA molecules were obtained from Takara Bio (Shiga, Japan). Two siRNA molecules were used, siBmi-1#1 and siBmi-1#2, with the targeted sequences 5′-AACAAUAACGAAUAGAAUUGA-3′ and 5′-AA GAAUUAUAACUGAUGAUGA-3′, respectively. Control (non-targeting sequence), unmodified siRNA duplex was also purchased from Takara Bio.

Statistical analysis. Data are expressed as mean ± SEM. The χ^2-test was used when appropriate to determine the correlations between clinicopathological variables and *Bmi-1* expression. The relative mRNA expression levels were compared using the unpaired *t*-test, and the Pearson's correlation coefficient test was also used. Statistical significance was defined as $P < 0.05$. All statistical analyses were carried out using Statcel software version 2.0 (OSM, Tokyo, Japan).

Results

***Bmi-1* expressed in HCC cell lines and distributed in high intensity, dot-pattern expression in nucleus.** To assess the potential role of *Bmi-1* in hepatocarcinogenesis, we examined *Bmi-1* expression in five human HCC cell lines using qRT-PCR and Western blot analysis. *Bmi-1* was highly expressed at both the mRNA and protein level. The most well differentiated HCC cell line, KIM-1, showed at least a three-fold higher level of expression of *Bmi-1*, compared with the other cell lines

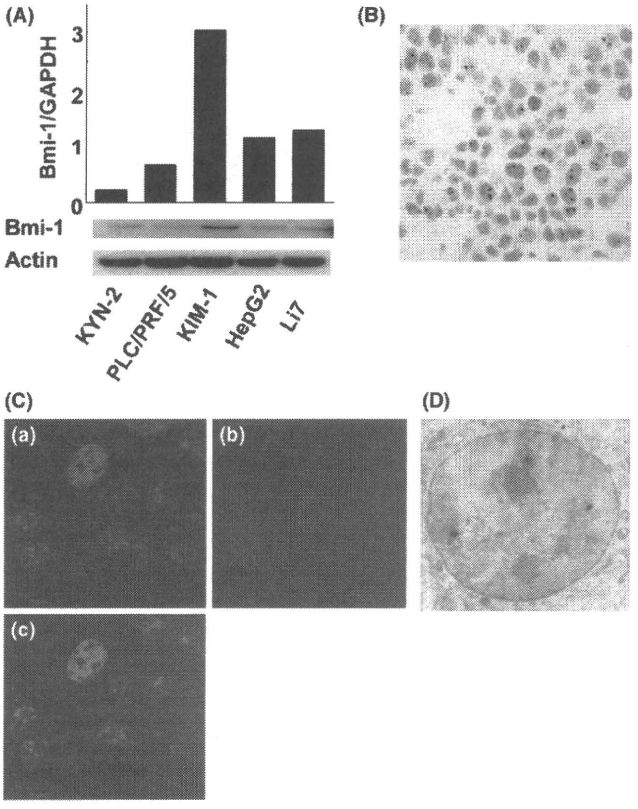

Fig. 1. *Bmi-1* expression in hepatocellular carcinoma (HCC) cell lines. (A) Quantitative real-time- PCR and Western blot of *Bmi-1* in HCC cell lines. *Bmi-1* is significantly expressed in the KIM-1 cell line compared with other cell lines. Nuclear fraction proteins were used in the Western blot analysis. Immunohistochemistry (B) and immuno cytochemistry (C) of KIM-1 cells. Bmi-1 was diffusely distributed intranuclearly (a, DAPI: blue; b, anti-Bmi-1: red; c, merged). (D) Immunoelectron micrograph of KIM-1. Bmi-1 particles are shown as small black dots inside the nucleus.

(Fig. 1A). As a transcriptional repressor, Bmi-1 activity is expected in the nucleus, and we found Bmi-1 protein enrichment in the nuclear fraction compared with the whole lysates (data not shown). Immunohistochemistry, immunocytochemistry, and immunoelectron microscopic of the KIM-1 cells showed that the Bmi-1 protein was distributed in high-intensity aggregates within the nucleus (Fig. 1B–D). These results confirmed localization of the Bmi-1 protein in the nucleus, with a dot-pattern appearance.

***Bmi-1* expressed in HCC clinical samples, particularly in early stage hepatocarcinogenesis.** We evaluated Bmi-1 protein expression in 122 HCC nodules (37 well differentiated [including 21 early nodules], 71 moderately, and 14 poorly differentiated HCCs). As with Bmi-1 expression in the HCC cell lines, Bmi-1 expression in clinical samples was observed as small dots distributed inside the nucleus (Fig. 2A), but the Bmi-1 dot-pattern expression was not observed in the surrounding liver tissue (Fig. 2B). There was no correlation between expression of Bmi-1 and clinicopathological parameters, such as age, gender, portal involvement, intrahepatic metastasis, etiology, or non-cancerous background liver tissue. However, Bmi-1 positive expression was significantly associated with well (including early) differentiated HCC ($P = 0.023$) (Table 1). A 2+ score was observed in 24 of the 37 (65%) well differentiated HCCs (including 13 of the 21 early nodules [62%]), 32 of the 71 (45%) moderately differentiated HCCs, and 7 of the 14 (50%) poorly differentiated HCCs. In contrast, negative expression was observed in only 2 of the 37 (5%) well differentiated HCCs (including 2 of the 21 early nodules [10%]), 15 of the 71 (21%) moderately differentiated HCCs, and 4 of the 14 (29%) poorly differentiated HCCs (Table 2). Interestingly, a higher level of Bmi-1 expression was observed in the early and well differentiated HCCs, and this declined with the progression of HCC. Similar findings were found using qRT-PCR from clinical tissue samples. Strongly positive *Bmi-1* expression was observed in the five well differentiated HCC cases, compared with the seven moderately differentiated cases and the three poorly differentiated HCC cases (Fig. 2C). The average level of *Bmi-1* expression was significantly higher in tumor tissue compared with the non-cancerous background liver tissue (2.23 *vs* 0.86; $P = 0.002$).

***Bmi-1* expression linked to *ABCB1* expression.** We have previously analyzed gene expression profiles after *Bmi-1* induction in bone marrow stromal cells.[6] Among the genes upregulated we found that the *ABCB1* gene was upregulated together with the overexpression of *Bmi-1*, compared with the control parental cells (T. Mori *et al.*, unpublished observation, 2004). To further verify the regulation of *ABCB1* we looked at changes in *ABCB1* expression during transient overexpression of *Bmi-1* using primary fetal hepatocytes. Following *Bmi-1* overexpression, relative mRNA levels of *ABCB1* in primary fetal hepatocytes were increased threefold (Fig. 3A). *Bmi-1* knockdown also led to a downregulation of *ABCB1* expression in the KIM-1 HCC cell line (Fig. 3B), however, decreased *ABCB1* expression was not very significant, which might be due to the presence of *Bmi-1*-independent *ABCB1* expression. These results suggest a parallel association between *Bmi-1* and *ABCB1* expression in HCC cell lines and hepatocytes.

***ABCB1* expression in HCC cell lines and HCC clinical samples correlated with *Bmi-1* expression.** We further evaluated *ABCB1* expression in HCC cell lines and clinical samples. As with *Bmi-1*, the highest levels of ABCB1 mRNA and protein expression were observed in KIM-1 cells, relative to the other cell lines. *ABCB1* mRNA expression level in tumor tissue is not significantly higher compared with non-cancerous background liver tissue due to its normal expression in non-cancerous background liver tissue, however, there is a tendency for higher expression level of *ABCB1* in well differentiated cases (2.30 *vs* 1.53; $P = 0.21$) (Fig. S1a,b). We found a strong statistical correlation between *ABCB1* and *Bmi-1* mRNA expression with the Pearson's correlation coefficient being 0.95 and 0.90 for HCC cell lines and HCC clinical samples, respectively (Fig. 4A,B). Immunohistochemical staining of ABCB1 showed both cytoplasmic and a canalicular staining pattern in the tumor region. Although the canalicular staining pattern was also seen in the surrounding non-cancerous region, the pattern was more irregular and thicker (Fig. S1c,d). A 2+ score was observed in 29 of 37 (78%) well differentiated HCCs (including 18 of 21 early differentiated nodules [86%]), in 50 of 71 (70%) moderately differentiated HCCs, and in 10 of 14 (71%) poorly differentiated HCCs. Negative expression was observed in 1 of 37 (3%) well differentiated HCCs (no early nodules had negative expression),

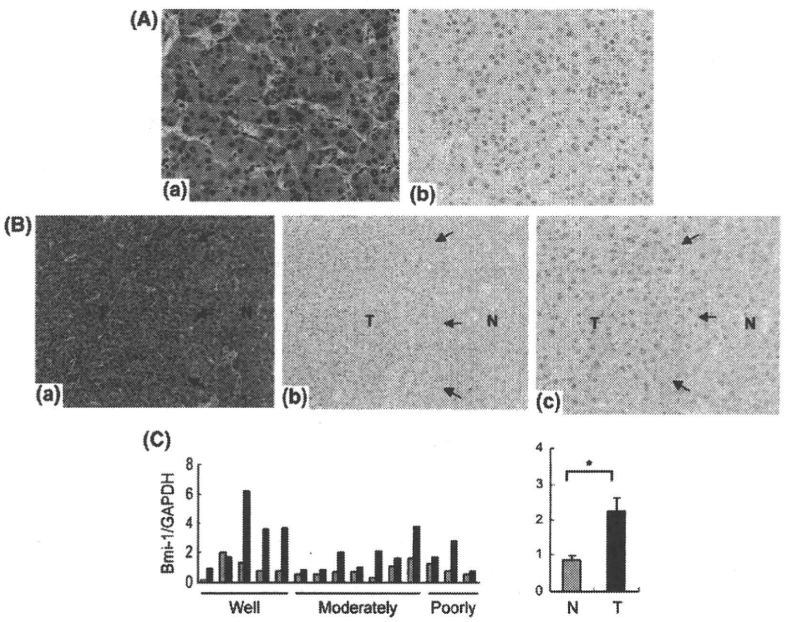

Fig. 2. *Bmi-1* expression in hepatocellular carcinoma (HCC) clinical samples. (A) Immunostaining of Bmi-1 in moderately differentiated HCC. Magnification, ×200. A clear dot-pattern of Bmi-1 was distributed diffusely in the tumor region. (B) Boundary region of well differentiated HCC (a, H&E stain; b, corresponding Bmi-1 staining, magnification ×100; c, magnification ×200). Bmi-1 expression was observed in the tumor region but not in surrounding liver tissue. Black arrows outline the border between the non-cancerous background region (N) and the tumor region (T). (C) *Bmi-1* mRNA expression levels in HCC clinical cases. The relative mRNA expression levels in tumor tissues (black bar, T) and corresponding non-cancerous, background liver tissues (gray bar, N) (left panel). High *Bmi-1* expression was observed in well differentiated HCC. The average expression level of *Bmi-1* was significantly higher in tumor tissues than in non-cancerous, background liver tissues (2.23 *vs* 0.86; $*P = 0.002$) (right panel).

doi: 10.1111/j.1349-7006.2009.01431.x

Table 1. Characteristics of 122 hepatocellular carcinoma nodules on the basis of Bmi-1 immunostaining

Characteristics	Bmi-1 expression		*P* value
	2+/1+	–	
No. of nodules	101	21	0.339
Mean age (years)	62.7	60.2	NA
Gender			
Male	88	15	NA
Female	13	6	
Tumor size (cm)			
<2	37	6	0.482
≥2	64	15	
Differentiation			
Well (early)	35 (19)	2 (2)	0.023*
Moderately/poorly	66	19	
Portal involvement			
–	54	9	0.376
+	47	12	
Intrahepatic metastasis			
–	80	14	0.214
+	21	7	
Etiology			
Hepatitis B virus	21	7	NA
Hepatitis C virus	61	12	
Non-B / Non-C	19	2	
Non-cancerous liver			
Liver cirrhosis	51	10	0.810
Others	50	11	

*$P < 0.05$. –, absence of dot-pattern staining; 1+, distributed focally with weak dot-pattern staining; 2+, distributed diffusely with clear dot-pattern staining; NA, not available.

Table 2. Immunohistochemical analysis of Bmi-1 expression in hepatocellular carcinoma (HCC) (n = 122)

Histology	Bmi-1 staining score		
	2+	1+	–
Well differentiated HCC (n = 37)	24 (65%)	11 (30%)	2 (5%)
Early HCC (n = 21)	13 (62%)	6 (29%)	2 (10%)
Moderately differentiated HCC (n = 71)	32 (45%)	24 (34%)	15 (21%)
Poorly differentiated HCC (n = 14)	7 (50%)	3 (21%)	4 (29%)

–, absence of dot-pattern staining; 1+, distributed focally with weak dot-pattern staining; 2+, distributed diffusely with clear dot-pattern staining.

in 5 of 71 (7%) moderately differentiated HCCs, and in 3 of 14 (21%) poorly differentiated HCCs (Table 3). As expected, ABCB1 expression was also higher in the well differentiated HCCs. There was a correlation in ABCB1 and Bmi-1 staining (Fig. 4C), and 50 of 122 (41%) cases showed strong expression of both Bmi-1 and ABCB1 (Table 4).

Discussion

Following the identification of *Bmi-1* overexpression in solid tumors,[9,14–16] some studies have also reported the overexpression of *Bmi-1* in HCC.[17,18,23] However, the *Bmi-1* localization area and whether *Bmi-1* is highly expressed in the early or late progression of HCC is still controversial. In this study, high levels of *Bmi-1* expression were observed in early HCC, and we carefully describe the specific subcellular expression of *Bmi-1* within the nucleus. We believe that as a transcriptional repressor, *Bmi-1* activity is expected to occur inside the nucleus.[10,24,25] Moreover, we found a correlation in the expression of *Bmi-1* and *ABCB1* suggesting that *ABCB1* might present a novel downstream target for *Bmi-1*.

Bmi-1 belongs to the Polycomb gene group (PcG) involved in maintaining target genes in their transcriptional state. A possible mechanism of PcG-mediated repression is the recruitment of certain regulatory factors, or chromatin-modifying activities, into a unique nuclear domain which results in inhibiting chromatin remodeling required for the transcriptional process.[24] Indeed, there is evidence showing that 3D imaging of PcG proteins in Drosophila embryos shows distribution of PcG complexes throughout the nuclear volume as discrete loci, which might reflect sites of repressive complexes.[25] In accordance with previous reports, we observed that *Bmi-1* was expressed as high-intensity, small aggregates distributed inside the nucleus in the HCC region. The *Bmi-1* dots appeared in different parts of the nucleus, often very near to or partially coincident with heterochromatin. These findings support the indication of *Bmi-1* function as a gene transcriptional repressor by regulating chromatin silencing. Regarding this immunohistochemical staining dot-pattern as a positive expression of *Bmi-1*, we found high levels of *Bmi-1* expression in well (included early) differentiated HCCs, whereas similar expression was not observed in the corresponding non-cancerous background hepatocytes.

The *Bmi-1* signaling pathway is one of the candidates that might, in part, govern stem cell fate, and acquirement of its "stemness" function has been linked to neoplastic proliferation.[4,26] The ability of *Bmi-1* to promote tumorigenesis and bypass senescence through regulation of *p16* and hTERT expression[6–9] suggests a potential role of *Bmi-1* in initiating hepatocarcinogenesis and immortalization of the hepatocyte.

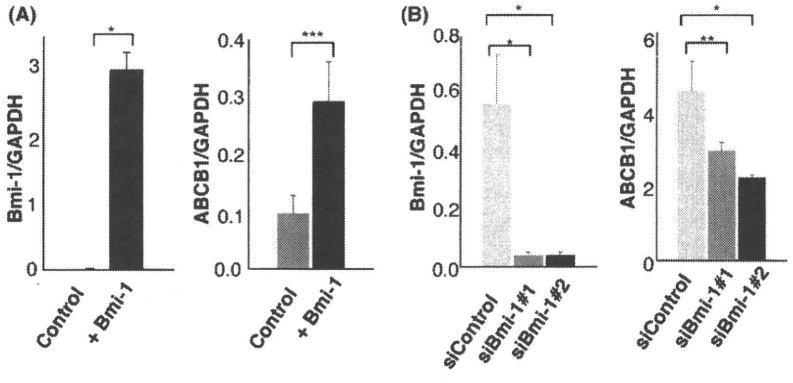

Fig. 3. Overexpression and silencing of *Bmi-1* expression affected ATP-binding cassette transporter B1 (*ABCB1*) expression in primary fetal hepatocytes and a hepatocellular carcinoma (HCC) cell line. (A) *Bmi-1* overexpression in primary fetal hepatocytes resulted in increased *ABCB1* expression, compared with the mock-transduced control (*$P < 0.01$; ***$P = 0.038$). (B) Silencing of *Bmi-1* expression by two different siRNAs (#1 and #2) in KIM-1 cells was followed by a decrease in *ABCB1* expression (*$P < 0.01$; **$P = 0.08$). Error bars were derived from three independent experiments.

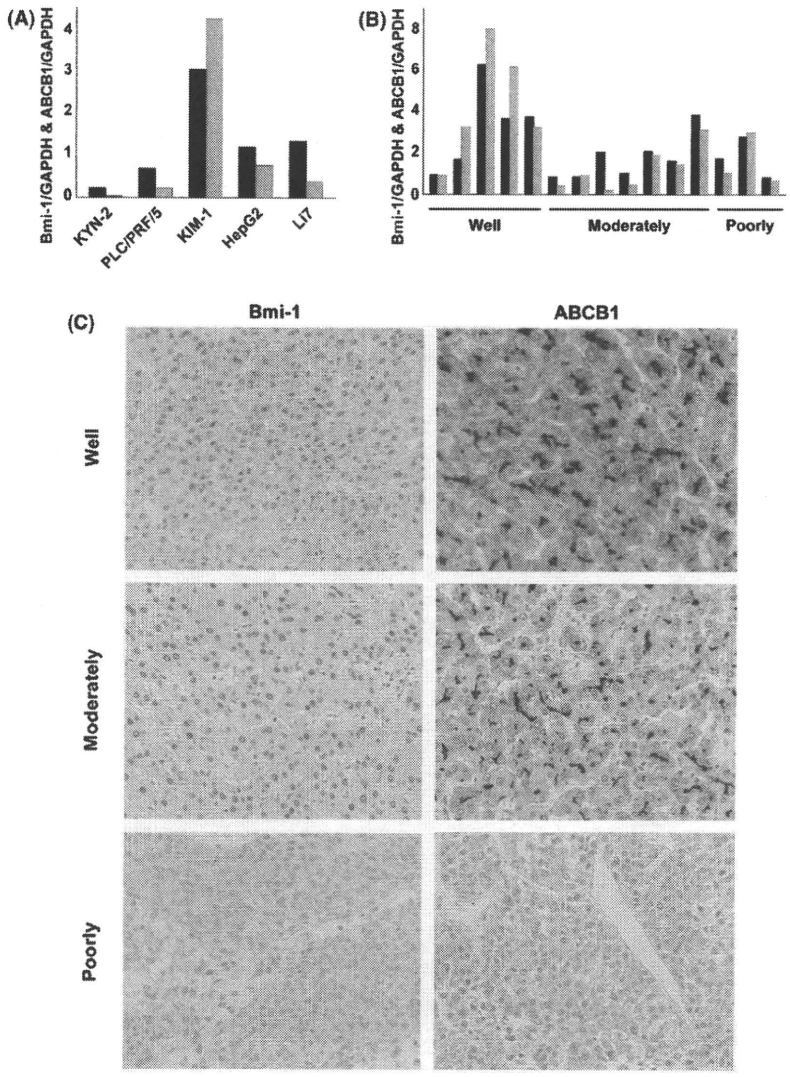

Fig. 4. Correlation and immunostaining of *Bmi-1* and ATP-binding cassette transporter B1 (*ABCB1*) expression in hepatocellular carcinoma (HCC). (A and B) Evaluation of *Bmi-1* and *ABCB1* mRNA expression in HCC cell lines and HCC clinical samples. A strong correlation between *Bmi-1* and *ABCB1* expression was observed in HCC cell lines and clinical samples by the Pearson's correlation coefficient test (0.95, $P = 0.01$; and 0.90, $P < 0.01$, respectively) (black column, *Bmi-1*; gray column, *ABCB1*). (c) Bmi-1 and ABCB1 expression in early, moderately, and poorly differentiated HCC (magnification, ×200). Clear staining of Bmi-1 "dot-pattern" (scored as 2+), and a canalicular and cytoplasmic ABCB1 staining pattern (scored as 2+), was observed in well differentiated HCC. Bmi-1 expression appeared weaker (scored as 1+), and only a canalicular staining pattern of ABCB1 (scored as 1+), was seen in moderately differentiated HCC. No dot-pattern of Bmi-1 and an absence of ABCB1 staining were observed in poorly differentiated HCC (scored as negative). Both Bmi-1 and ABCB1 expression decreased with the progression of HCC, suggesting their correlated expression.

Table 3. Immunohistochemical analysis of ATP-binding cassette transporter B1 (ABCB1) expression in hepatocellular carcinoma (HCC) (n = 122)

Histology	ABCB1 staining score		
	2+	1+	–
Well differentiated HCC (n = 37)	29 (78%)	7 (19%)	1 (3%)
Early HCC (n = 21)	18 (86%)	3 (14%)	0 (0%)
Moderately differentiated HCC (n = 71)	50 (70%)	16 (23%)	5 (7%)
Poorly differentiated HCC (n = 14)	10 (71%)	1 (7%)	3 (21%)

–, no staining; 1+, irregular canalicular staining pattern; 2+, clear staining of irregular canalicular with cytoplasmic staining.

Table 4. Combined immunohistochemical analysis of *Bmi-1* and ATP-binding cassette transporter B1 (ABCB1) expression in hepatocellular carcinoma

ABCB1 staining score Bmi-1 staining score	2+	1+	–
2+	50 (41%)	12 (10%)	1 (1%)
1+	28 (23%)	7 (6%)	3 (2%)
–	11 (9%)	5 (4%)	5 (4%)

ABCB1 staining scores: –, no staining; 1+, irregular canalicular staining pattern; 2+, clear staining of irregular canalicular with cytoplasmic staining. Bmi-1 staining scores: –, absence of dot-pattern staining; 1+, distributed focally with weak dot-pattern staining; 2+, distributed diffusely with clear dot-pattern staining.

Low levels of *p16* expression and increased activation of hTERT have also been reported in HCC, including in early HCC.[19,27,28] We observed high levels of *Bmi-1* expression in early HCC, which might indicate an indispensable function for *Bmi-1* in the early development of cancer. *Bmi-1* expression was also observed in progressed HCC, however, the expression level was not as high as in early HCC. This findings suggested *de novo* tumor development pathways as well as indicated another functional role of *Bmi-1* in progressed HCC. Although it is clear that *Bmi-1* plays a role in keeping self-renewal ability and proliferation, the exact molecular mechanism of *Bmi-1* in early hepatocarcinogenesis remains unclear. Inactivation of *p16* expression by methylation or epigenetic mechanisms has already been observed as an early

doi: 10.1111/j.1349-7006.2009.01431.x